Nature and utility of auditory steady state response as a translational science tool for neuropsychiatric disorders

(精神神経疾患におけるトランスレーショナルサイエンスツールとしての聴性定常反応の特徴と有用性)

Graduate School of Comprehensive Human Sciences
University of Tsukuba

Naoki Kozono

Table of Contents

Abstract

While significant unmet medical needs persist for patients with neuropsychiatric disorders, there are yet to be any effective treatments and new drugs have failed to be developed. The repeated failures suggest the need for further research into translatable biomarkers bridging of patients in preclinical models. The gamma oscillation of auditory steady-state response (ASSR) has recently been proposed as a biomarker for neuropsychiatric disorders, including schizophrenia and fragile X syndrome (FXS). However, the stable and strict recording of ASSR to click stimuli with two indices of inter-trial coherence (ITC) and event-related spectral perturbation (ERSP) is less well defined in preclinical model as compared with clinics. The present study aims to establish novel recording methods for ASSR in rats and validate it both with pharmacological response (chapter I) and genetic disease model (chapter II). We developed here novel methods using a switchable pedestal which allows electroencephalography (EEG) recording at whatever two brain regions of interest, e.g. temporal and parietal cortex. EEG recording at the temporal cortex with the pedestal enabled distinct detection of clearer ASSR signals both with ERSP and ITC, and the 40 Hz ASSR showed maximal as observed in humans. The constructed recording methods of ASSR enabled to well characterize both pharmacodynamic response to *N*-methyl-D-aspartate receptor (NMDAR) antagonist and EEG phenotypes of disease animal model. The NMDAR antagonist, ketamine exerted a bi-phasic effect on ASSR in gamma bands while increasing the basal gamma power in wild type (WT) rats. *Fmr1*-targeted transgenic rats, FXS model rats, displayed robust attenuation of ASSR ERSP and ITC at gamma bands and enhanced basal gamma power, consistent with findings in subjects with FXS. These findings demonstrated that ASSR gamma power signals can be well recorded with the constructed recording methods in

rodents, which allows us to study pharmacological responses and disease phenotype as observed in human. Further study with this system will uncover the more detailed mechanism of ASSR, potentially enabling to investigate new drugs for neuropsychiatric disorders as a translational biomarker.

Abbreviations

Nonstandard abbreviations were listed in alphabetical order.

ADME	absorption, distribution, metabolism, and excretion
ANOVA	analysis of variance
AP	anteroposterior
ASSR	auditory steady-state response
ECoG	electrocorticogram
EEG	electroencephalography
E/I	excitation/inhibition
ERP	event-related potential
ERSP	event-related spectral perturbation
FFT	fast Fourier transform
FMRP	fragile X mental retardation protein
FMR1	*fragile X mental retardation 1*
Fmr1-KO rats	*fmr1*-targeted transgenic rats
FXS	fragile X syndrome
GABA	gamma-aminobutyric acid
ISI	inter-signal interval
ITC	inter-trial coherence
ITI	inter-trial interval
KO	knock out
ML	mediolateral
NMDAR	*N*-methyl-D-aspartate receptor

PK/PD	pharmacokinetic/pharmacodynamic
PLF	phase locking factor
PV	parvalbumin
SEM	standard error of the mean
VD	ventral depth
WT	wild type
ZFN	zinc finger nuclease

General introduction

While significant unmet medical needs persist for patients with neuropsychiatric disorders, there are few effective treatments and development of new drugs have failed [1, 2]. Failures of new investigational drugs are largely due to failing to reach primary endpoints set in clinical trials. The repeated failures of new investigational drugs for neuropsychiatric disorders emphasize the need for further research into translatable biomarkers, i.e. how to predict the clinical efficacy based on the preclinical models [1, 3, 4].

Electroencephalography (EEG) is an indirect technique to measure neuronal activity in the brain and is widely used in the research of neurology, cognitive science, and psychophysiology. The auditory steady-state response (ASSR) has been used to study auditory temporal processing and has recently been proposed as an EEG biomarker for neuropsychiatric disorders, including schizophrenia and fragile X syndrome (FXS) [3, 5, 6]. The entrainment of ASSR is generally defined by two indices with time-frequency decomposition (General Fig. 2A); inter-trial coherence (ITC) and event-related spectral perturbation (ERSP) [7]. ITC indicates phase consistency across trials (0; complete phase shifts, 1; completely synchronized phase) and could more directly reflect neural synchrony. ERSP is defined as an event-related response relative to pre-stimulus baseline power based on amplitudes, meaning that it would be affected by alteration in baseline gamma power. The potent ASSR signal has been reported at parietal cortex (vertex, Cz) and/or midline frontal areas (Fz) [6, 8-11], although the source of human ASSR has been extensively studied and found to originate in the primary auditory cortex based upon the various methods [12-15]. However, which brain regions are responsible for ASSR signals in rodents remains elusive since the stable and strict recording of rodent

ASSR in electrocorticogram (ECoG) is less well defined, considering reports of ASSR from various brain regions such as the prefrontal cortex [16] and auditory cortex [17, 18]. In addition, the recording method of ASSR to click sound stimuli to detect both ERSP and ITC from the brain surface has not been standardized in preclinical studies. Therefore, the novel methods enabling for EEG to record at two brain regions of interest were constructed and validated, which allows to compare the ASSR signals recorded at two brain regions between temporal and parietal cortex (Fig. 1 in chapter I).

ASSR-based research focuses on not only relatively low-frequency oscillations (1–30 Hz) but also higher-frequency oscillations in the gamma band (30–200 Hz) (General Fig. 2B) [3, 7]. Measurement of gamma oscillation is generally performed in one of two ways. Basal (resting) gamma measures native gamma oscillations in the absence of external stimuli. In contrast, evoked (time-locked) gamma is passive gamma oscillation elicited by auditory stimuli. The gamma oscillation is closely linked to various neuropsychiatric disorders, including schizophrenia [7, 19-21] and FXS [5, 22] which debilitating neurodevelopmental disorder caused by a CGG repeat expansion mutation in the *fragile X mental retardation 1* (*FMR1*) gene on the X chromosome [23]. Studies of gamma frequency oscillation at 40 Hz have demonstrated differences between schizophrenic patients and normal controls [7, 20]. Moreover, the cortical oscillatory activity contributes to sensory hypersensitivity and social communication deficits in FXS, and that ASSR at gamma frequencies is reduced in FXS [5, 22, 24].

Numerous studies suggest that changes in gamma oscillation likely reflect the a ctivity of parvalbumin (PV) positive gamma-aminobutyric acid (GABA) interneuron populations which plays an important role in sensory input processing [25, 26]. I t is hypothesized that alterations in gamma oscillations are indicative of an imbal ance in excitation/inhibition (E/I) arising from the loss of function within the abov

e-mentioned interneuron population. The blunting *N*-methyl-D-aspartate receptor (NMDAR) signaling transduction in PV positive interneurons increases basal gamma power, while decreases evoked gamma power [26, 27]. The NMDAR antagonist, decreases persistent firing of pyramidal neurons, affecting neuronal synchrony and disrupting ASSR [18, 28]. The ketamine at 30 mg/kg induced a biphasic effect on phase locking factor (PLF) of 40 Hz ASSR based on pharmacokinetic/pharmacodynamic (PK/PD) response with NMDA receptor occupancy [16]. *Fmr1*-targeted transgenic rats (*Fmr1*-KO rats) were recently established by Sage Laboratories, LLC, using zinc finger nuclease (ZFN) technology to target exon 8 of the *Fmr1* gene as a preclinical model of FXS [29]. *Fmr1*-KO rats showed decrease of fragile X mental retardation protein (FMRP) expression derived from a 122 bp deletion in *Fmr1* gene and displays disrupted cortical processing of auditory stimuli [30]. Forebrain excitatory neuron selective deletion of the *fmr1* gene leads to reduction of density of PV cells and enhancement of basal EEG gamma power [31]. Therefore, ASSR and basal power at gamma frequency bands was assessed in NMDA receptor antagonist treatment or *Fmr1*-KO rats, which induce E/I imbalance.

Present study measured the cortical gamma oscillatory responses to validate the constructed methods of ASSR with both pharmacological response by NMDAR antagonist (chapter I) and phenotypes in *Fmr1*-KO rats (chapter II).

General figures

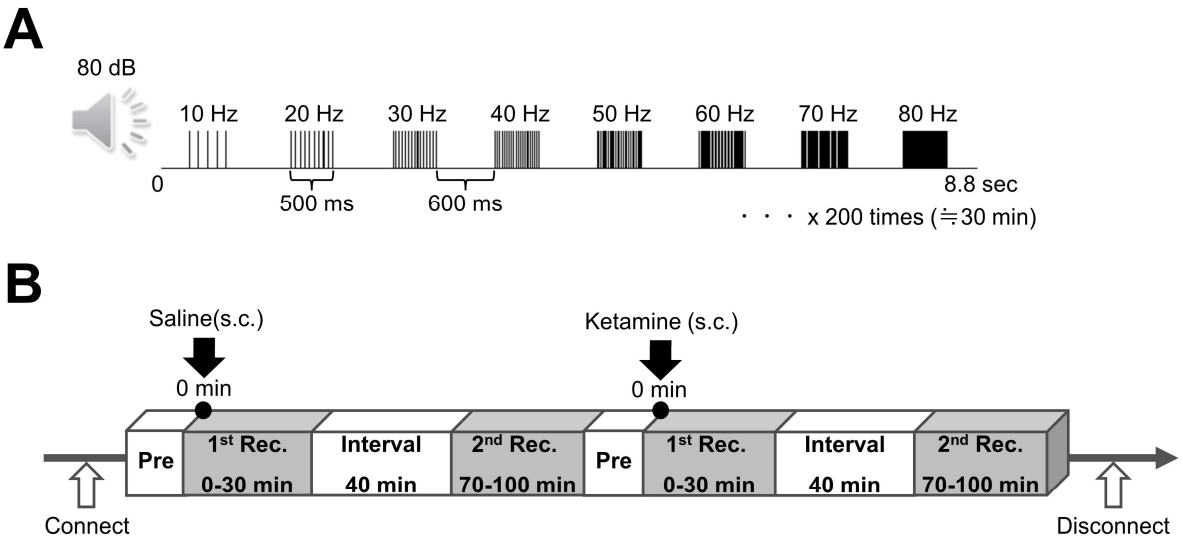

Fig. 1.

Fig. 1. Graphical representation of the experimental paradigm of auditory steady-state response (ASSR) recording. (A) A schematic of the protocol for ASSR recording (Rec.). Auditory stimuli consisted of click sounds (80 dB) which include 500 msec trains at 10, 20, 30, 40, 50, 60, 70, and 80 Hz. Click sounds trains at each frequency were repeated 200 times/trial for approximately 30 min with 600 msec of the inter-trial interval (ITI) and inter-signal interval (ISI). (B) A schematic of the procedure for long-term ASSR recording in chapter I. Following subcutaneous (s.c.) injection of saline or ketamine at time zero, rats were exposed to auditory sound stimuli at 0–30 min (1st Rec.) and 70–100 min (2nd Rec.), and the electroencephalography (EEG) data were recorded from parietal or temporal cortex (duration of collection indicated by gray rectangular boxes).

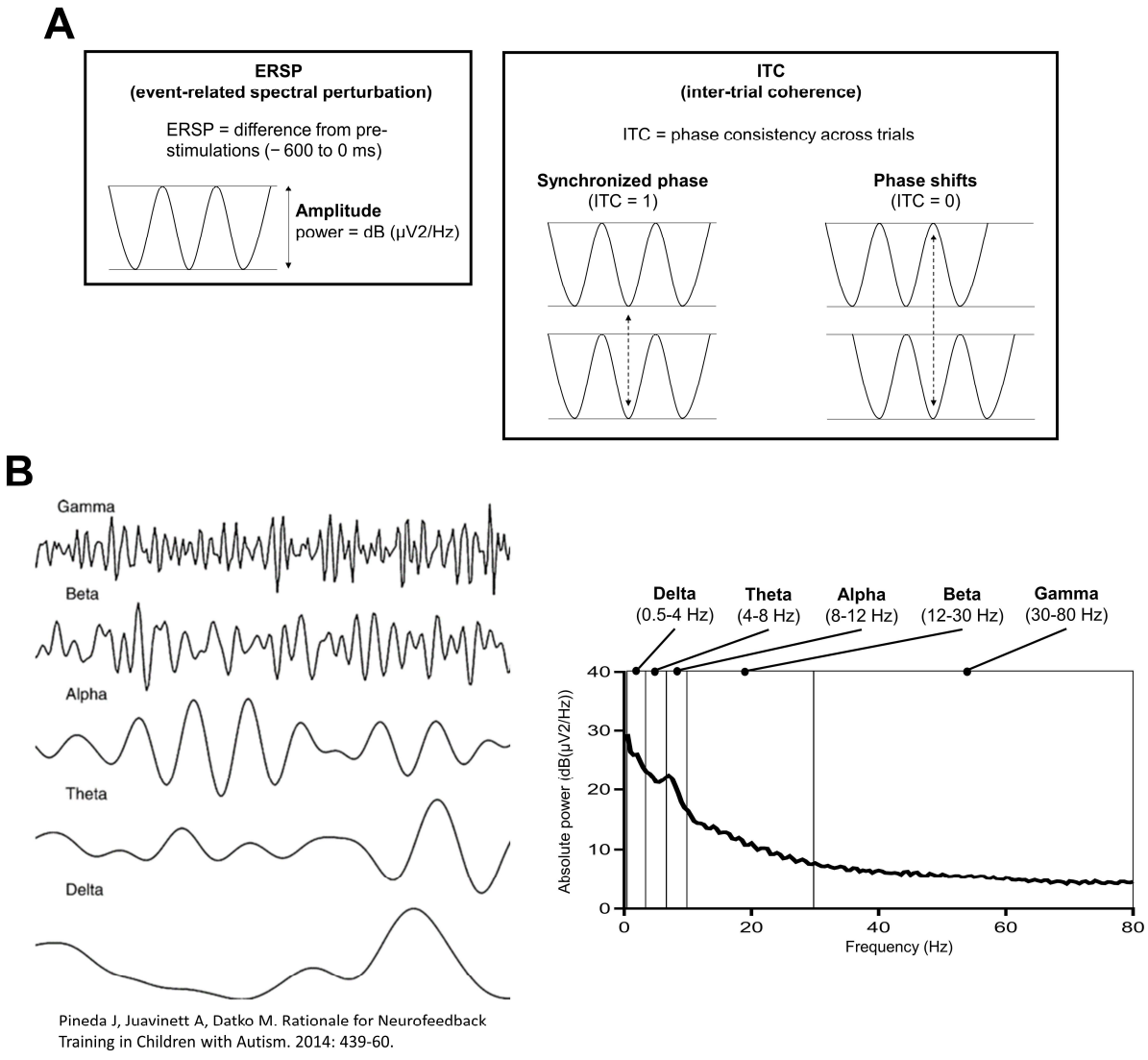
A
ERSP
(event-related spectral perturbation)
ERSP = difference from pre-stimulations (− 600 to 0 ms)
Amplitude
power = dB (µV2/Hz)
ITC
(inter-trial coherence)
ITC = phase consistency across trials
Synchronized phase
(ITC = 1)
Phase shifts
(ITC = 0)
B
Gamma
Beta
Alpha
Theta
Delta
Delta
(0.5-4 Hz)
Theta
(4-8 Hz)
Alpha
(8-12 Hz)
Beta
(12-30 Hz)
Gamma
(30-80 Hz)
Absolute power (dB(µV2/Hz))
Frequency (Hz)
0
10
20
30
40
0
20
40
60
80
Pineda J, Juavinett A, Datko M. Rationale for Neurofeedback Training in Children with Autism. 2014: 439-60.

Fig. 2.

Fig. 2. Graphical representation of the recording parameters in electroencephalography (EEG) recording. (A) auditory steady-state response (ASSR) defined by two indices with time-frequency decomposition; inter-trial coherence (ITC) indicating phase consistency across trials (0; complete phase shifts, 1; completely synchronized phase) and event-related spectral perturbation (ERSP) indicating event-related difference in the power spectrum based on amplitudes. (B) Visual representations of the most common EEG at each frequency band in reference and power spectrum. Basal power was calculated at delta (0.5–4 Hz), theta (4–8 Hz), alpha (8–12 Hz), beta (12–30 Hz) and gamma (30–80 Hz) frequency bands in present study.

Chapter I

Auditory Steady State Response;
nature and utility as a translational science tool

Summary

The ASSR has been used to detect auditory processing deficits in patients with psychiatric disorders. However, the methodology of ASSR recording from the brain surface has not been standardized in preclinical studies, limiting its use as a translational biomarker. The sites of maximal ASSR in humans are the vertex and/or middle frontal area, although it has been suggested that the auditory cortex is the source of the ASSR. I constructed and validated novel methods for ASSR recording using a switchable pedestal which allows ASSR recording alternatively from temporal or parietal cortex with a wide range of frequencies in freely moving rats. I further evaluated ASSR as a translational tool by assessing the effect of ketamine. The ASSR measured at parietal cortex did not show clear ERSP or ITC in any frequency bands or a change with ketamine. In contrast, the ASSR at temporal cortex showed clear ERSP and ITC where 40 Hz was maximal in both gamma band frequencies. Ketamine exerted a biphasic effect in ERSP at gamma bands. These findings suggest that temporal cortex recording with a wide frequency range is a robust methodology to detect ASSR, potentially enabling application as a translational biomarker in psychiatric and developmental disorders.

Introduction

EEG-detectable event-related potential (ERP) analysis can reveal sensory processing deficits in patients with psychiatric disorders [6]. The ASSR has been used to study auditory temporal processing, hearing screening [32], and to monitor the state of arousal during anesthesia [33]. Recently, ASSR has been proposed as a biomarker for psychiatric disorders such as schizophrenia [6] and developmental disorders [5].

The source of human ASSR has been extensively studied and found to originate in the primary auditory cortex based upon the dipole model [11, 13-15, 34], the LORETA model [14, 15], and independent component analysis [12]. However, potent ASSR signal has been reported at the vertex and/or midline frontal areas [8-11, 35-37]. The difference between the highly-responsive brain regions and the generation source region for ASSR are easily reconciled due to the fact that ECoG signal is based on volume conduction [38]. In rodents, the evidence supporting auditory cortex as the ASSR origin region is based on direct implanted electrode recording from multiple brain areas [39]. However, the stable and strict recording of rodent ASSR in ECoG is less well defined considering reports of ASSR from various brain regions such as the prefrontal cortex [16], and auditory cortex [17, 18]. I hypothesized that more precise region-specific analysis would reveal specific electrophysiological phenotypes that could be applied as non-invasive biomarkers for translational studies. The analysis focused on the parietal and temporal cortex based upon anatomical features of the rat cranium and theory of volume conduction. The application of a novel switchable pedestal enabled recording from these two brain regions from the same rat and consequently resulted in direct power comparison by region (Figure 1).

Classical auditory ERP analysis produces a signature pattern of time-dependent

positive (P1, etc) and negative (N1, etc.) deflections from baseline. The latency or amplitude of these signature peak events can be robustly modulated with tool compounds such as the widely-studied NMDAR antagonist, that can reduce ERP such as N1 amplitude in both clinical and preclinical studies [40, 41]. Through antagonizing NMDAR in the prefrontal cortex, persistent firing of pyramidal neurons can be reduced, affecting neuronal synchrony and disrupting ERP [28]. However, ketamine induced a biphasic effect on ITC of 40 Hz ASSR in the prefrontal cortex based on the PK/PD response [16]. Note that the efficacy of ketamine on ERSP in rat ASSR has not been previously reported. The synchronies of ASSR might be influenced by not only the gamma oscillation but also the ERPs. Furthermore, NMDAR antagonism showed the frequency-specific enhancement of ITC in ASSR with four different stimulation frequencies [42]. The current study utilized a wide range frequency stimulus of ASSR to evaluate neural synchronization [43]. ASSR with various different stimulation has been used successfully to drive and examine neural activity across a wide frequency range in healthy volunteers [43, 44], and in case-control studies for schizophrenia [45]. Further, these ASSR are sensitive to pharmacological manipulation [46]. Therefore, I also assessed the effect of ketamine over a broad range of ASSR (ERSP and ITC) frequencies in two brain areas using a switchable pedestal to establish the novel methods as a bridge between rats and humans and thus test its utility as a tool for translational and reverse-translational approach between preclinical and clinical studies.

Materials and Methods

Animals

Sprague-Dawley rats were purchased (Charles River Laboratories Japan, Inc., Ishioka, Japan). The sixteen rats were housed in temperature- and humidity-controlled rooms (23 ± 2 °C and 55 ± 10%) under a 12-h light/dark cycle with free access to water. Recording were performed in dim light (<300 lux). All animal experimental procedures were performed in accordance with Guide for the Care and Use of Laboratory Animals, 8th edition and approved by the Institutional Animal Care and Use Committee of Astellas Pharma Inc. Furthermore, Astellas Pharma Inc., Tsukuba Research Center was awarded Accreditation Status by the AAALAC International.

Surgery

I created an original electrode pedestal which can switch the acquisition position between temporal cortex or parietal cortex (Fig. 1A) and customized electrode cables (Fig. 1B) in cooperation with S.E.R. Corporation (Shinagawa-ku, Tokyo, Japan). Design details can be made available upon request. Before 8 weeks of age, rats underwent anchor screw attachment into the skull (no contact with the meninges) at the following coordinates: temporal cortex (Anteroposterior: AP −4.5 mm, Mediolateral: ML −7.5 mm, Ventral depth: VD −4.0 mm), vertex (AP −1.0 mm, ML −1.0 mm, parietal cortex), frontal sinus for reference (AP 8.0 mm, ML −1.5 mm) and cerebellum for ground (AP −10.0 mm, ML −1.5 mm) under anesthesia using 2–2.5% isoflurane (Fig. 1C). The stainless steel wires were attached to the switchable pedestal by soldering at each terminals (Fig. 1C). The switchable pedestal with stainless steel wire electrodes were attached to the cranium using methacrylic resin (Repairsin, GC Corporation, Bunkyo–ku, Tokyo, Japan). After

surgery, the rats were housed singly and had unrestricted access to food and water.

Drugs

Ketamine hydrochloride (50 mg/mL, Daiichi Sankyo Co., Ltd, Tokyo, Japan) was diluted with saline. Ketamine (30 mg/2 mL/kg) or saline were subcutaneously (s.c.) administered to all rats in a final volume of 2 ml/1 kg body weight.

EEG recording

EEG recording was performed using a programming script with a data acquisition and analysis software package (Spike2, Cambridge Electronic Design: CED, Milton, Cambridge, UK). Rats were hooked to customized electrode cables up to the switchable pedestal, selecting the temporal cortex or parietal cortex with ground and reference (Fig. 1D). The electrode cables were connected to high-impedance differential AC amplifier (Sampling rate; 1000 Hz, Low Cut-Off Filter: 1 Hz, High Cut-Off Filter: 500 Hz, model #1800, A-M Systems, Carlsbrog, WA, US) and versatile data acquisition unit (Micro1401, CED). Rats were individually placed into recording boxes in a faraday cage with speakers attached to the cage top, and freely moved during the EEG recording (Fig. 1E). For habituation, the ASSR recording was started at least 30 min after placement in the recording box. Auditory stimuli consisted of click sounds (80 sound decibels: dB) which include 500 msec trains at 10, 20, 30, 40, 50, 60, 70, and 80 Hz (General Fig. 1A). Click sounds trains at each frequency were repeated 200 times/trial, the inter-trial interval (ITI) and inter-signal interval (ISI) was 600 msec. Rats were exposed to auditory sound stimuli at 0–30 (1st recording) and 70–100 min (2nd recording) automatically by the programming script after saline administration, and the EEG data were recorded from parietal or temporal cortex (General Fig. 1B). After that consecutively,

rats were treated with ketamine and were re-exposed to the auditory sound stimuli. At least one week without recording was applied to all rats as a withdrawal term between recordings from parietal or temporal cortex.

Data analysis

The EEG data from Spike2 were converted to a Matlab environment. By using EEGLAB on a MATLAB toolbox (MathWorks, Natick Massachusetts, USA), the files were split into each trial (200 times), all outliers in each split file were rejected for movement artifact based on a criterion of 2 times root mean squared amplitude per mouse. In ASSR analysis, low-pass filter (100 Hz) was applied to the EEG data to remove artifacts. The mean number of epochs for each group were as follows: parietal (saline at 1st recording: 181, ketamine at 1st recording: 186, ketamine at 2nd recording: 180), temporal (saline at 1st recording: 183, ketamine at 1st recording: 188, ketamine at 2nd recording: 179). Averaging stimuli during each click sound trains were calculated by wavelet transformation (frequency limits: 8 to 100 Hz, wavelet cycles:10 to 62.5, epoch size: 9.0 sec). As output data, the measurable factors were divided into two different data; ERSP (baseline: pre-stimulations from −600 to 0 msec) and ITC on a MATLAB toolbox and were gathered by open source software, KNIME (KNIME AG, Zurich, Switzerland) (General Fig. 2A). By using same split files, spectrum analysis was performed and calculated by the fast Fourier transform (FFT) analysis (baseline: pre-stimulations) on MATLAB toolbox. The value during 30–80 Hz were derived from power of spectrum as gamma power (General Fig. 2B).

Statistics

Statistical analysis for ASSR between the parietal cortex group and the temporal cortex

group, or saline group and ketamine group, was conducted using two-way repeated measures analysis of variance (ANOVA) followed by Bonferroni multiple comparison test (GraphPad Prism 7, GraphPad Software, San Diego CA, USA). Statistical analysis for basal gamma power between saline group and ketamine group was conducted using paired t-test.

Results

Comparison between parietal and temporal cortex recordings of ASSR

In time-frequency plots, the ASSR from the temporal cortex showed higher ERSP and ITC, whereas neither ERSP nor ITC from the parietal cortex recording showed a clear response (Fig. 2A,B). ASSR between parietal and temporal cortex showed a statistically significant difference by a two-way repeated measures ANOVA with frequency (ERSP; $F(7, 105) = 6.632$; $P < 0.01$, ITC; $F(7, 105) = 14.34$; $P < 0.01$), and by electrode position (ERSP; $F(1, 15) = 33.83$; $P < 0.01$, ITC; $F(1, 15) = 41.75$; $P < 0.01$). ASSR from temporal cortex showed significantly higher responses than the parietal cortex in both ERSP (10–50 Hz) and ITC (10–60 Hz). In the gamma band frequency, 40 Hz ASSR showed the most robust response in both ERSP and ITC, although ITC in 20 Hz ASSR showed the maximal response of all frequencies measured (Fig. 2C,D).

Biphasic alteration of ERSP or ITC in ASSR from temporal cortex recording by ketamine dosing

The alteration of ERSP and ITC by ketamine were recorded at 1st recording (0–30 min) or 2nd recording (70–100 min) after administration at time t = 0 min. In ERSP recording, results were derived from multiple comparison after two-way repeated measures ANOVA with frequency (1st recording; $F(7, 105) = 15.28$; $P < 0.01$, 2nd recording; $F(7, 105) = 29.51$; $P < 0.01$), treatment (1st recording; $F(1, 15) = 7.806$; $P < 0.05$, 2nd recording; $F(1, 15) = 55.88$; $P < 0.01$). In ITC recordings, results were derived from multiple comparison after two-way repeated measures ANOVA with frequency (1st recording; $F(7, 105) = 30.85$; $P < 0.01$, 2nd recording; $F(7, 105) = 23.75$; $P < 0.01$), treatment (1st recording; $F(1, 15) = 2.012$; $P = 0.1765$, 2nd recording; F (1,

15) = 80.56; P < 0.01), and frequency × treatment (1st recording; F (7, 105) = 9.095; P < 0.01, 2nd recording; F (7, 105) = 28.84; P < 0.01). Ketamine (30 mg/kg) altered ERSP and ITC in both recording (Figs 3A,B, 4A,B). In the 1st recording, ketamine significantly reduced ERSP at 40, 50, 60, and 70 Hz compared with saline, used here as a solvent control for ketamine (Fig. 3C). ERSP at 10, 20, 30, 40, 50, and 70 Hz significantly increased at 2nd recording after ketamine treatment (Fig. 3D). On the other hand, ITC significantly increased at 10, 30, and 40 Hz in 1st recording by ketamine treatment although ITC at 20 Hz was significantly reduced (Fig. 4C). In the 2nd recording, ketamine significantly increased ITC at 10, 20, 30, 40, 50, 60 and 70 Hz compared with saline (Fig. 4D).

The alteration of ASSR from parietal cortex recording by ketamine administration

Ketamine did not alter ERSP in both recording of ASSR recording from parietal cortex after two-way repeated measures ANOVA with frequency (1st recording; F (7, 105) = 0.8242; P = 0.57, 2nd recording; F (7, 105) = 3.136; P < 0.01), treatment (1st recording; F (1, 15) = 5.203; P < 0.05, 2nd recording; F (1, 15) = 0.405; P = 0.53) (Fig. 5A,C). In the ITC recording, results were derived from multiple comparison after two-way repeated measures ANOVA with frequency (1st recording; (F (7, 105) = 10.8; P < 0.01, 2nd recording; F (7, 105) = 26.91; P < 0.01), treatment (1st recording; F (1, 15) = 52.92; P < 0.01, 2nd recording; F (1, 15) = 0.205; P = 0.66), and frequency × treatment (1st recording; F (7, 105) = 9.986; P < 0.01, 2nd recording; F (7, 105) = 11.8; P < 0.01). ITC during 1st recording showed significant reduction at 30 and 40 Hz (Fig. 5B,D). These reductions of ITC remained in the 2nd recording with significant reduction at 50 Hz although ITC at 20 and 30 Hz was significantly increased by ketamine treatment. However, the basal power of gamma frequency bands (30–80 Hz) was significantly

increased at the temporal cortex as well as parietal cortex in both recordings after ketamine administration (Fig. 6A,B).

Discussion

The innovative feature of this study is that constructed switchable pedestal enabled recording from both parietal and temporal cortex in the same rat without restraint. This enabled us to probe suitable recording position for rat ASSR and establish the potential for application of ASSR as a translational biomarker. The robust response from rat temporal cortex in the 40 Hz range is consistent with ASSR in human [43]. From this wide-range ASSR paradigm, both shared and unique features between preclinical and clinical assessments were discovered. The temporal cortex recording of ASSR produced a biphasic effect of ketamine on ERSP/ITC while the parietal recording from the same animals did not.

Temporal cortex recording in ECoG enables neuronal synchronization of ERSP and ITC

ASSR recording from the temporal cortex revealed significantly higher ERSP and ITC at frequency of 10–50 Hz compared to values recorded from the parietal cortex. Supporting this, Wang et al suggested that ASSR recording from the auditory cortex showed the highest response by comparison with other brain regions such as prefrontal cortex and hippocampus, among others [39]. Prior studies reported clear ERSP in rat ASSR [17, 42]. However, ECoG recording methods significantly contribute to this literature by enabling detection of both ERSP and ITC from temporal cortex. In contrast, the parietal recording of ASSR produced unclear ERSP and ITC. I first clarified the different responses of ERSP and ITC in these regions in rodent. However, potent response of ASSR were detected at the vertex and/or midline frontal areas in clinical studies [8-11, 35-37]. The difference of the high-response region might be derived from shape and/or volume differences of the brain between rats and human because volume conduction effects enable ECoG recording

[38]. Indeed, threshold differences in bone-conduction ASSR between post-term infants and adults has been suggested to be due to skull maturation [11, 47]. By using the switchable pedestal, I revealed the detectable signal from rat ASSR in temporal cortex, and difference of ASSR between rats and human. These results shown here emphasize the utility of present methodology for the basic science of ASSR.

Frequency characteristics of ASSR in preclinical and clinical investigations

The wide-range frequency of ASSR setup enables clarification of common and divergent features between preclinical and clinical studies. Common features include the peak ERSP and ITC responses at 40 Hz in the gamma band in rat and human ASSR [43, 45]. Divergent features include the highest ITC at 20 Hz and smallest ERSP and ITC at 80 Hz in rat which were not consist with the clinical reports although the same results were reported in rat ASSR [42]. These shared and unique features indicate that ASSR can be a powerful translatable biomarker, but that care must be taken to select the most informative frequencies for stimulation and response.

Alternation of ASSR over broad frequencies by ketamine administration

Ketamine at 30 mg/kg in rat significantly decreased the ERSP at 40–70 Hz in the 1st recording. However, the response to ketamine was inverted significantly in the 2nd recording. I first revealed the biphasic effect at gamma bands in ASSR from temporal cortex recording. This result is consistent with a previous report that observed biphasic responses in 40 Hz ASSR despite recording from Fz [16]. Ketamine altered both amplitude and latency in auditory ERPs as a shared feature between clinical and preclinical studies [40, 41]. This effect of ketamine might be caused by the persistent reduction of neuronal firing of inter neurons, i.e. GABAergic neurons, in the cortex [6, 28,

48]. Thus, ketamine might directly influence the mode of action by which gamma oscillation is developed in ASSR. It has been suggested that lower exposure of ketamine (like 2nd recording in present study) biases the excitatory/inhibitory balance toward increased excitability [16]. However, the effect of ketamine on ASSR could not be only explained by the inhibition of neuronal firing, because it produced biphasic responses across a wide range of gamma band frequency. Indeed, higher exposure of ketamine (1st recording) reduced both ERSP and ITC of ASSR. This may reflect a collapse of cortical neuronal synchrony. However, it is necessary to investigate this result at a deeper mechanistic level to better understand the dose- and time-dependent differential responses as they could simply be caused by a specific efficacy of ketamine such as dissociative anesthesia.

Studies of gamma frequency oscillation (40 Hz) have demonstrated differences between schizophrenic patients and normal controls [7, 20, 49]. One conclusion from these studies is that inappropriate regulation of fast-spiking cortical GABAergic interneurons results from NMDA hypofunction. The present study showed reduction of the 40 Hz ERSP consistent with schizophrenia patients and robustly affected the ERSP and ITC at 30 and 40 Hz by ketamine. In addition, augmentation of ASSR at 40 Hz in the 2nd recording was also consistent with clinical observations [50]. These results indicate that our recording methods enabled to detect high similarity of ASSR in schizophrenia patients and robust alteration of gamma oscillations.

This methodology also revealed that the augmented ERSP and ITC at 10 Hz ASSR by ketamine remained in both recordings. To the best of knowledge, there are no previous reports demonstrating that ketamine affects 10 Hz ASSR in both preclinical and clinical experimental systems. NMDAR antagonist altered ERPs in both clinical and preclinical studies [40, 41] and basal power of alpha bands (8–12 Hz) in clinical studies [51]. This

could reflect a causal relationship among ERPs, basal power and ASSR, but further investigation is warranted.

ASSR recording from parietal cortex did not show a robust biphasic effect of ketamine on ERSP and ITC. However, the basal power in the gamma frequency was significantly increased in parietal cortex recording as well as temporal cortex recording by ketamine in the same rat. A previous report also suggested that 30 mg/kg ketamine steadily augmented gamma power in frontal cortex [52], suggesting that the exposure level of ketamine in this study is suitable for producing neurophysiological responses. Thus, the switchable pedestal with a wide range of frequencies of sound stimuli revealed that the rat ASSR has not only regional differences but also differences of drug responses. Through direct intracranial comparison of candidate brain regions, sampling a broad range of input stimuli frequencies and output response frequencies, the current study identified the temporal (preclinical) and parietal/Fz (clinical) as a suitable brain regions and 40 Hz a tractable frequency for translational studies linking informative features of rat electrophysiological response to standard noninvasive measurements of human clinical response to drug. Further investigation by using the novel device described here to test hypotheses in additional brain areas such as the prefrontal cortex will provide insights into the mechanism of ASSR, and its interpretation/validation as a translatable biomarker.

The critical need for more predictive human biomarkers of neuroleptic drug efficacy is matched by a need for preclinical experimental systems that accurately reflect the human condition. Multiple consortia of academic research teams and federal programs are driving toward the application of human EEG/ERP as clinical biomarkers. These include the Bipolar Schizophrenia Network on Intermediate Phenotypes (BSNIP) project at National Institute of Mental Health (NIMH), ERP Biomarker Qualification

Consortium, Brain Mapping by Integrated Neurotechnologies for Disease Studies (Brain/MINDS) project [53-55]. Outside of the basic research domain and in the context of neuroleptic drug development, there will be a growing need for corresponding preclinical experimental systems that provide a clear line of sight from drug discovery through development. This work takes an important step toward harmonizing ASSR as a translational tool toward achieving this ambitious end.

Conclusions

I constructed and validated novel methods for ASSR recording by using a switchable pedestal which allows ASSR recording at the temporal cortex or parietal cortex with a wide range of frequencies in same freely moving rat. As the results, ASSR recording at the temporal cortex enabled distinct detection of ERSP and ITC with each auditory click train stimuli, and that the 40 Hz ASSR shows maximal ERSP and ITC, similar to humans. Ketamine exerted a bi-phasic effect in gamma bands (40–70 Hz). These responses and effects were not clearly detected in ASSR recordings from parietal cortex in the same rats. Thus, ASSR recordings from the temporal cortex have high validity as a preclinical ASSR model. From these findings, this constructed switchable recording and wide-range ASSR paradigm are useful for basic science and novel drug development as a forward and backward translational science tool.

Figures

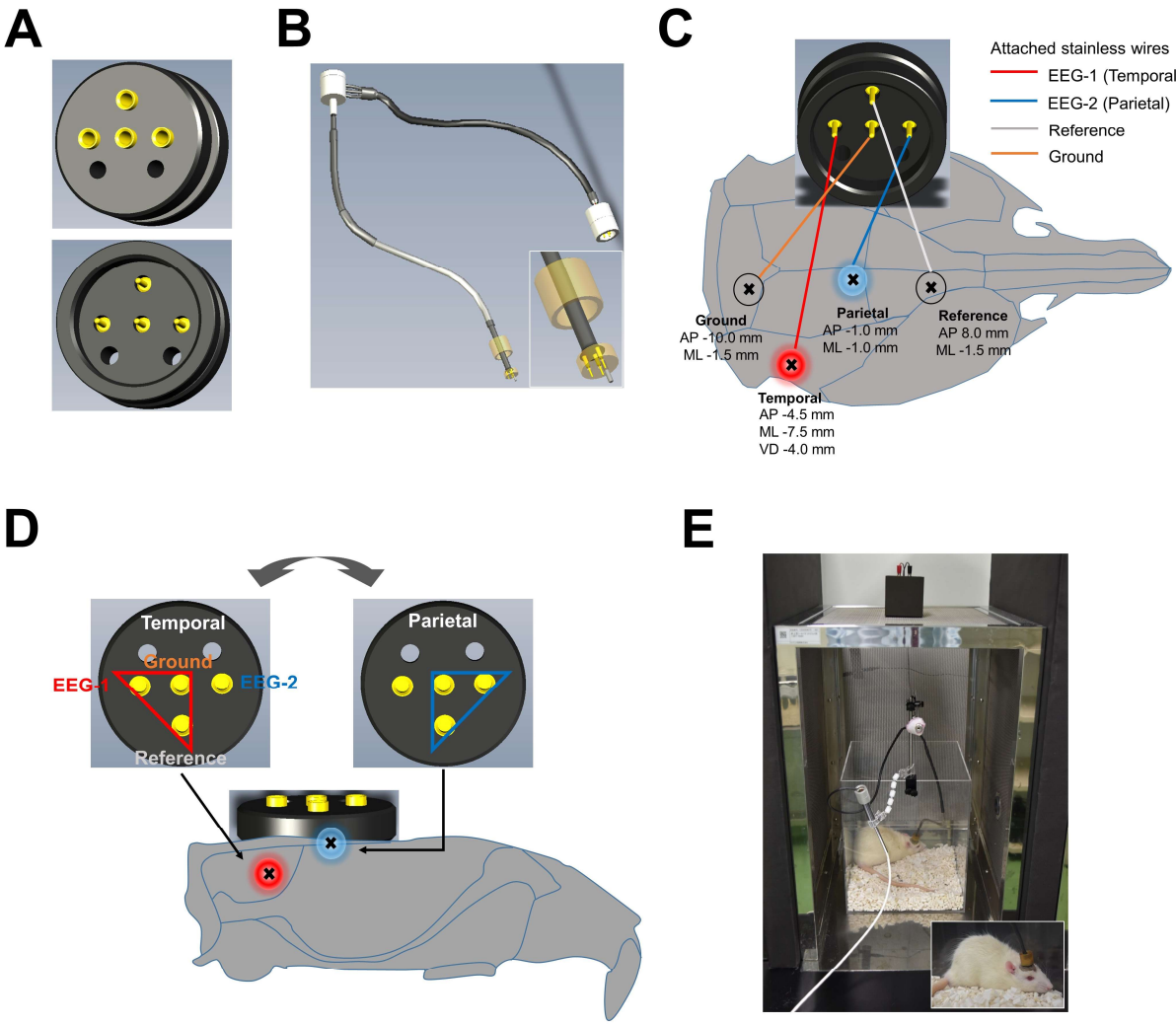

Fig. 1.

Fig. 1. The switchable pedestal which can record from temporal or parietal cortex in the same rat. (A) The original switchable pedestal with 4 terminals. (B) The customized electrode cables to connect with pedestal. White box shows enlarged illustration of connector pin which attaches to each terminal in the pedestal. (C) The anchor screw was put into the skull of rats at the following coordinates: temporal cortex (Anteroposterior: AP −4.5 mm, Mediolateral: ML −7.5 mm, Ventral depth: VD −4.0 mm), parietal cortex (AP −1.0 mm, ML −1.0 mm), frontal sinus for reference (AP 8.0 mm, ML −1.5 mm) and cerebellum for ground (AP −10.0 mm, ML −1.5 mm). The stainless steel wires were attached to the pedestal by soldering at the following position: temporal cortex (red line), parietal cortex (blue line), ground (orange line) and reference (gray line) displayed on the figure. (D) The recording position of auditory steady-state response (ASSR) was switchable between temporal and parietal cortex. On the temporal cortex, customized electrode cables were hooked up with electroencephalography (EEG)-1, ground and reference (red triangle). On the parietal cortex, customized electrode cables were hooked up with EEG-2, ground and reference (blue triangle). (E) Rats were individually placed into a recording box in faraday cage with speakers attached to the cage top, and freely moving during the EEG recording. White box shows enlarged figure of rat with attached electrodes during ASSR recording.

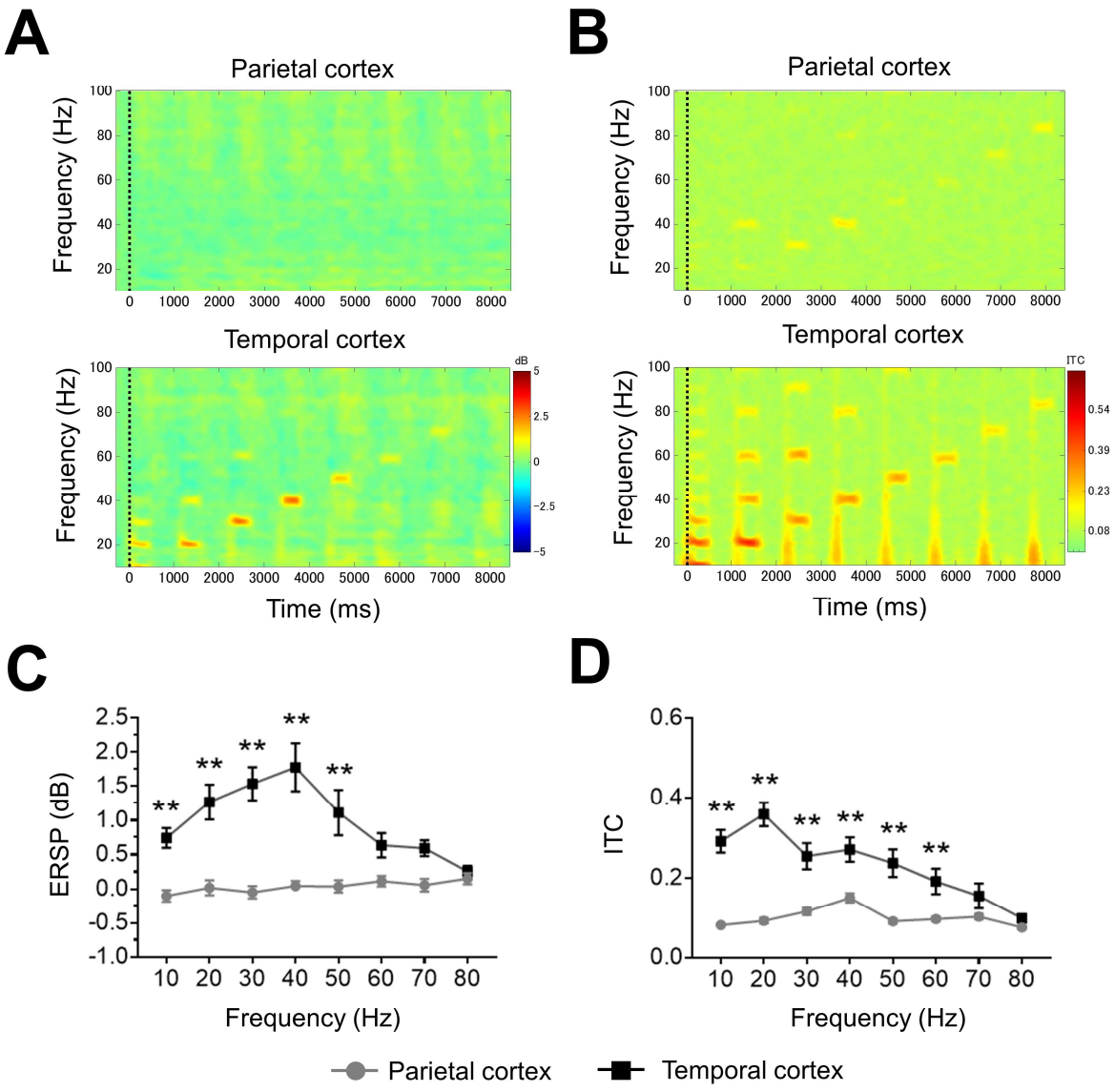
A
Parietal cortex
Frequency (Hz)
Temporal cortex
dB
Time (ms)
B
Parietal cortex
Frequency (Hz)
Temporal cortex
ITC
Time (ms)
C
ERSP (dB)
Frequency (Hz)
D
ITC
Frequency (Hz)
Parietal cortex
Temporal cortex

Fig. 2.

Fig. 2. The comparison of auditory steady-state response (ASSR) recording between parietal and temporal cortex. (A) The time-frequency plots of event-related spectral perturbation (ERSP) at parietal (top) and temporal cortex (bottom). (B) The time-frequency plots of inter-trial coherence (ITC) at parietal (top) and temporal cortex (bottom). In time-frequency plots, warmer color (reds, yellows) indicate higher ERSP or ITC. (C) The ERSP (10–80 Hz) at parietal (circle line) and temporal cortex (square line). (D) The ITC (10–80 Hz) at parietal (circle line) and temporal cortex (square line). Data represent mean ± SEM (n = 16). **p < 0.01, significant differences between the groups; two-way repeated measures ANOVA followed by Bonferroni multiple comparison test.

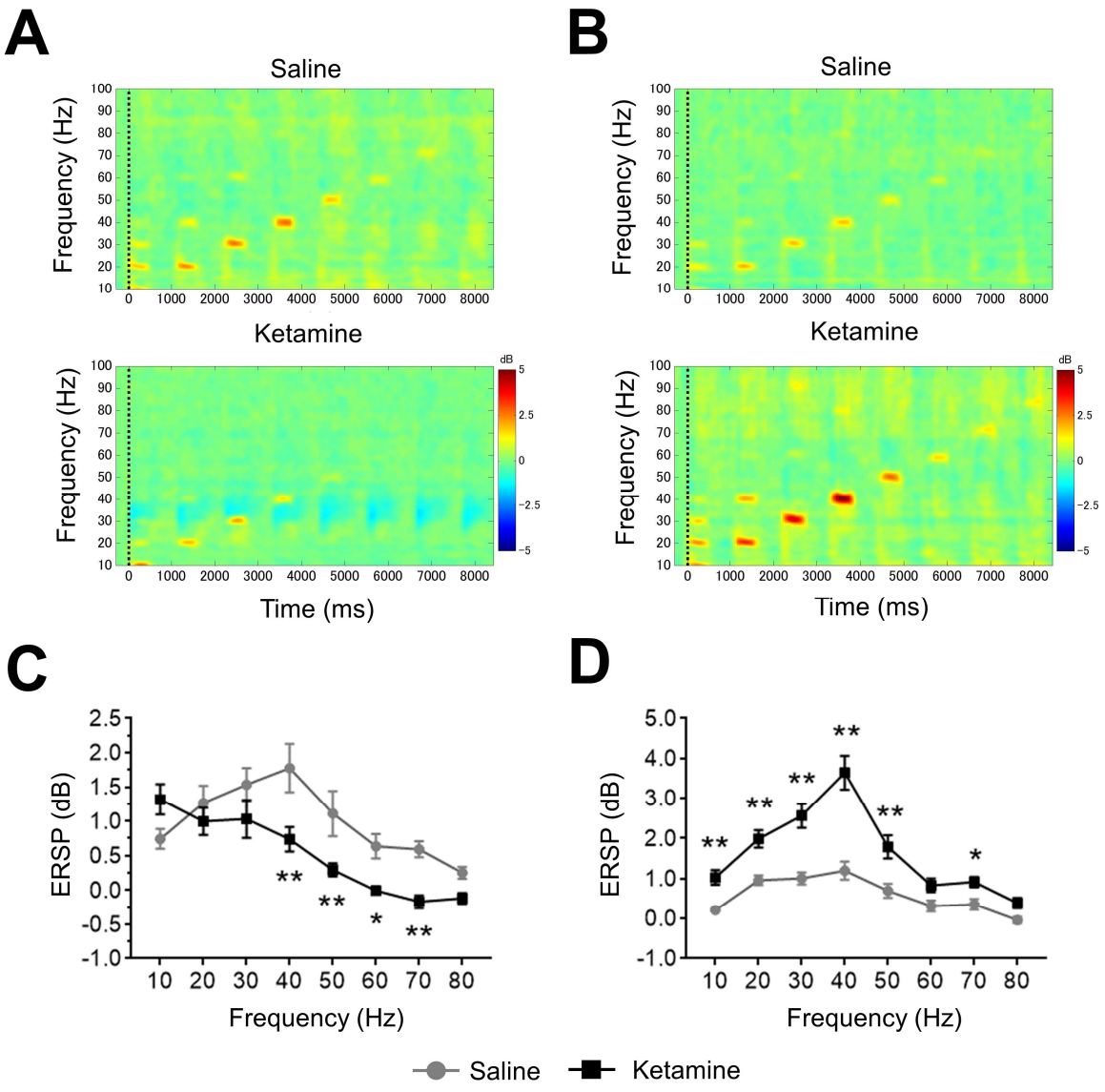
A
Saline
Frequency (Hz)
Ketamine
Time (ms)
B
C
ERSP (dB)
Frequency (Hz)
D
Saline
Ketamine

Fig. 3.

Fig. 3. The effect of ketamine on event-related spectral perturbation (ERSP) from temporal cortex recording. (A) The time-frequency plots of ERSP at 1st recording (0–30 min) after saline (top) and ketamine (bottom) administration. (B) The time-frequency plots of ERSP at 2nd recording (70–100 min) after saline (top) and ketamine (bottom) administration. In time-frequency plots, warmer color (reds, yellows) indicate higher ERSP. (C) The ERSP (10–80 Hz) at 1st recording after saline (circle line) and ketamine (square line) administration. (D) The ERSP (10–80 Hz) at 2nd recording after saline (circle line) and ketamine (square line) administration. Data represent mean ± SEM (n = 16). *p < 0.05, **p < 0.01, significant differences between the groups; two-way repeated measures ANOVA followed by Bonferroni multiple comparison test.

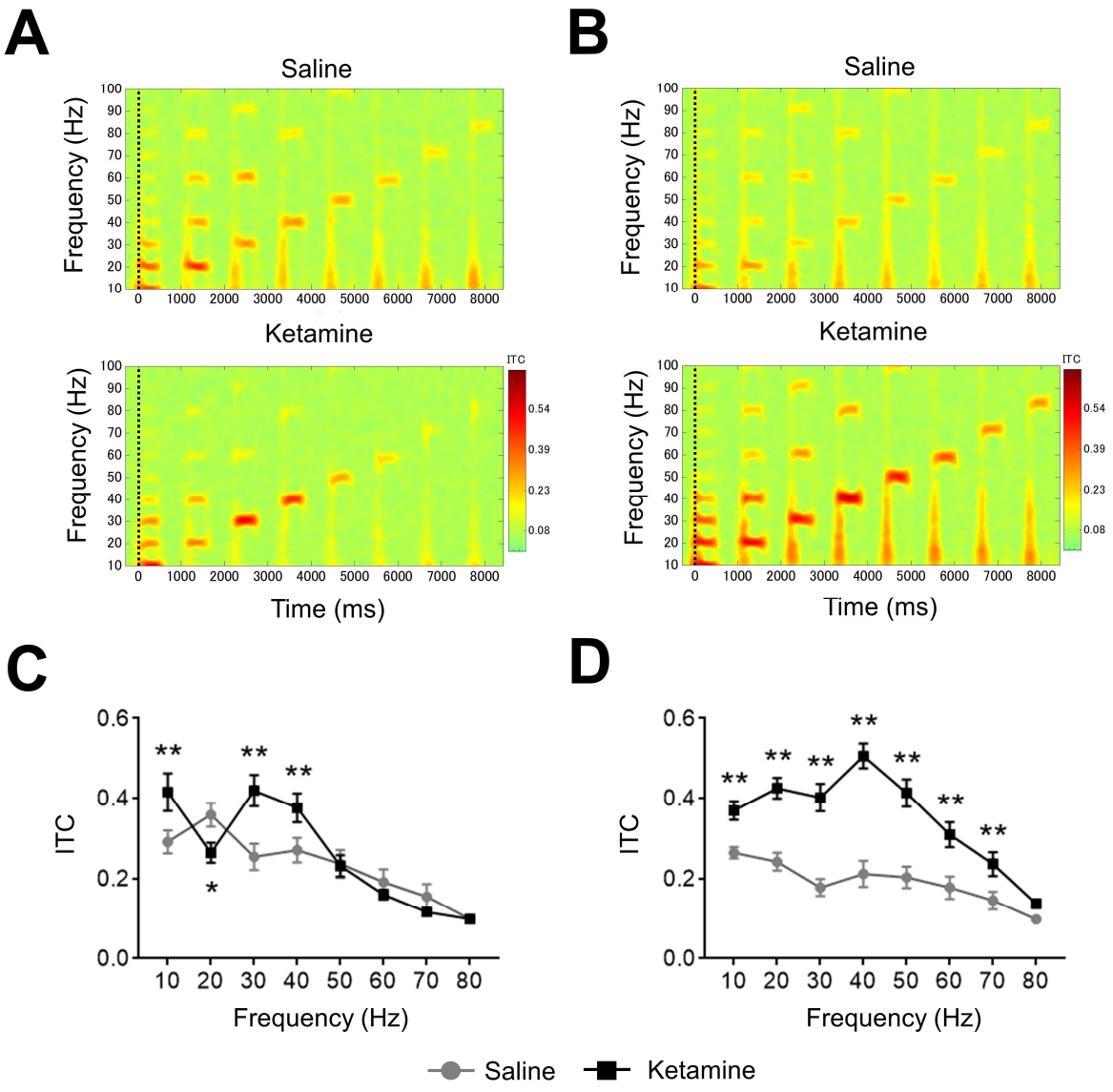
A
Saline
Frequency (Hz)
Ketamine
ITC
Time (ms)
B
C
ITC
Frequency (Hz)
D
Saline
Ketamine

Fig. 4.

Fig. 4. The effect of ketamine on inter-trial coherence (ITC) from temporal cortex recording. (A) The time-frequency plots of ITC at 1st recording (0–30 min) after saline (top) and ketamine (bottom) administration. (B) The time-frequency plots of ITC at 2nd recording (70–100 min) after saline (top) and ketamine (bottom) administration. In time-frequency plots, warmer color (reds, yellows) indicate higher ITC. (C) The ITC (10–80 Hz) at 1st recording after saline (circle line) and ketamine (square line) administration. (D) The ITC (10–80 Hz) at 2nd recording after saline (circle line) and ketamine (square line) administration. Data represent mean ± SEM (n = 16). *p < 0.05, **p < 0.01, significant differences between the groups; two-way repeated measures ANOVA followed by Bonferroni multiple comparison test.

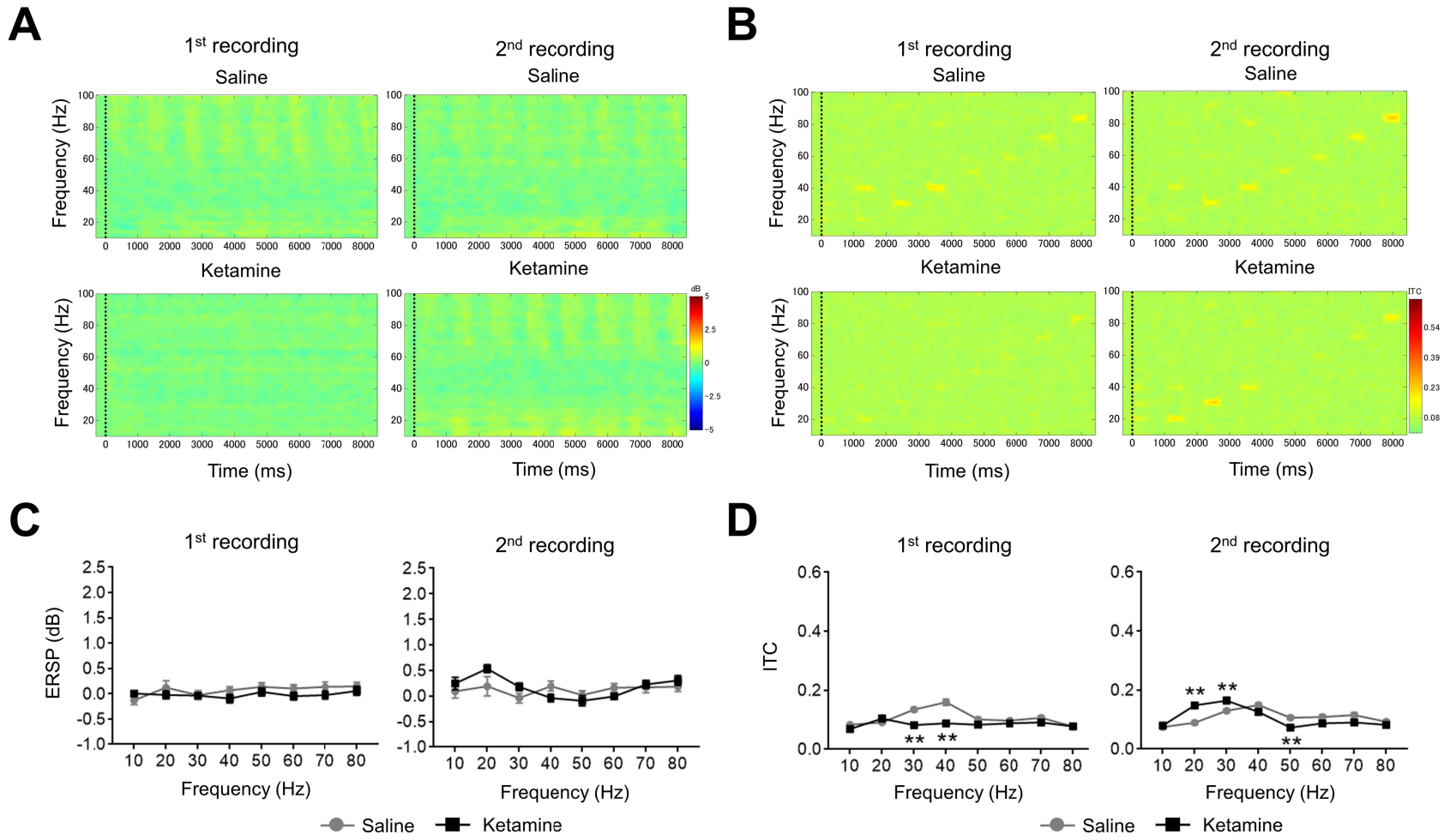
A
1st recording
Saline
2nd recording
Saline
Ketamine
Ketamine
Frequency (Hz)
Time (ms)
dB
B
1st recording
Saline
2nd recording
Saline
Ketamine
Ketamine
Frequency (Hz)
Time (ms)
ITC
C
1st recording
2nd recording
ERSP (dB)
Frequency (Hz)
Saline
Ketamine
D
1st recording
2nd recording
ITC
Frequency (Hz)
Saline
Ketamine

Fig. 5.

Fig. 5. The effect of ketamine on auditory steady-state response (ASSR) from parietal cortex. (A) The time-frequency plots of event-related spectral perturbation (ERSP) at 1st recording (0–30 min) and 2nd recording (70–100 min) after saline (top) and ketamine (bottom) administration. (B) The time-frequency plots of inter-trial coherence (ITC) at 1st recording (0–30 min) and 2nd recording (70–100 min) after saline (top) and ketamine (bottom) administration. In time-frequency plots, warmer color (reds, yellows) indicate higher ERSP and ITC. (C) The ERSP (10–80 Hz) at 1st recording and 2nd recording after saline (circle line) and ketamine (square line) administration. (D) The ITC (10–80 Hz) at 1st recording and 2nd recording after saline (circle line) and ketamine (square line) administration. Data represent mean ± SEM (n = 16). **p < 0.01, significant differences between the groups; two-way repeated measures ANOVA followed by Bonferroni multiple comparison test.

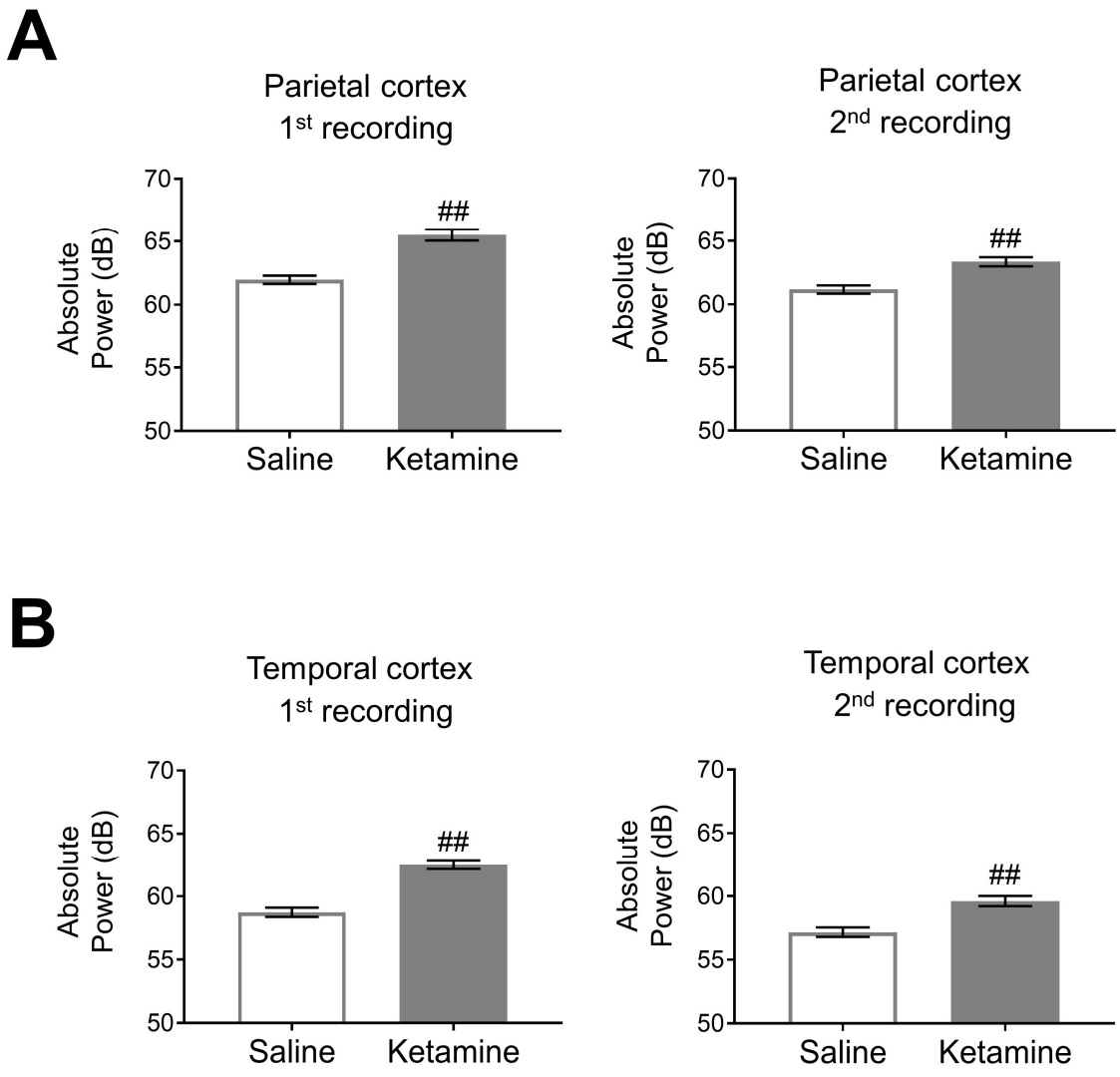

Fig. 6.

Fig. 6. The effect of ketamine on basal power of gamma frequency bands (30–80 Hz). (A) The absolute low gamma power (30–80 Hz) at 1st recording or 2nd recording after saline (left) or ketamine administration (right) in parietal cortex. (B) The absolute low gamma power at 1st recording or 2nd recording after saline (left) or ketamine administration (right) in temporal cortex. Data represent mean ± SEM (n = 15–16). ##$p < 0.01$, significant differences between the groups; paired t-test.

Chapter II

Gamma power abnormalities in a *Fmr1*-targeted transgenic rat model of fragile X syndrome

Summary

FXS is characteristically displayed intellectual disability, hyperactivity, anxiety, and abnormal sensory processing. EEG abnormalities are also observed in subjects with FXS, with many researchers paying attention to these as biomarkers. Despite intensive preclinical research using *Fmr1* knock out (KO) mice, an effective treatment for FXS has yet to be developed. Here, I examined *Fmr1*-KO rats as an alternative preclinical model of FXS. I characterized the EEG phenotypes of *Fmr1*-KO rats by measuring basal EEG power and ASSR to click trains of stimuli at a frequency of 10 to 80 Hz. *Fmr1*-KO rats exhibited reduced basal alpha power and enhanced gamma power, and these rats showed enhanced locomotor activity in novel environment. While ASSR clearly peaked at around 40 Hz, both ITC and ERSP were significantly reduced at the gamma frequency band in *Fmr1*-KO rats. *Fmr1*-KO rats showed gamma power abnormalities and behavioral hyperactivity that were consistent with observations reported in mouse models and subjects with FXS. These results suggest that gamma power abnormalities are a translatable biomarker among species and demonstrate the utility of *Fmr1*-KO rats for investigating drugs for the treatment of FXS.

Introduction

FXS is a debilitating neurodevelopmental disorder caused by a CGG repeat expansion mutation in the *FMR1* gene on the X chromosome [23] that results in loss of the FMRP. FXS is estimated to affect 1 in 4000 men and 1 in 8000 women [56], and patients are characterized by intellectual disability, hyperactivity, anxiety, seizures, autism-like symptoms, and abnormal sensory processing [57, 58]. Auditory processing deficits are also a common feature in subjects with FXS [22, 59-61]. Further, EEG abnormalities are observed in 74% of males with FXS, and hyperactivity, a major behavioral symptom of FXS, is observed in 50–66% [62]. EEG abnormalities in subjects with FXS are usually characterized by an enhancement in the amplitude of the N1 of the ERP in response to auditory stimuli [59, 63-65] and basal gamma power [5, 22, 24]. Furthermore, recent evidence suggests that cortical oscillatory activity contributes to sensory hypersensitivity and social communication deficits in FXS [22, 24], and that ASSR at gamma frequencies is reduced in FXS [5], the abnormalities that is widely used as a translational biomarker in neuropsychiatric disorders such as schizophrenia [6] and developmental disorders [66].

Fmr1 KO mice have been used as a preclinical model of FXS for more than 20 years [67]. Complete loss of FMRP causes neuronal morphological alterations such as changes to spine shape and density [68, 69], and behavioral abnormalities such as hyperactivity and hypersensitivity to sensory stimuli [29, 70]. Note that EEG abnormalities are observed in preclinical mice models. *Fmr1* KO mice show blunted ASSR at the gamma frequency band, like that observed in subjects with FXS [71]. Thus, EEG measures appear to be a useful translational biomarker for drug development for FXS.

Despite intensive research into the pathophysiology of FMRP for more than a decade, there are yet to be any effective treatments of FXS patients [67]. Over 10 diverse

interventions have failed or showed only minimal effects in clinical trials, despite preclinical studies having indicated various benefits of these interventions in *Fmr1* KO mice [1]. Thus, evidence from *Fmr1* KO mice alone may not be sufficient to warrant clinical investigation. Lessons learned from past drug developments for FXS suggest the need for further research into translatable biomarkers using mice of different genetic backgrounds (C57BL/6 or FVB) or other disease models [1, 66, 67].

In 2014, *Fmr1*-KO rats were established by Sage Laboratories, LLC (Emmett, I D, USA), using ZFN technology to target exon 8 of the *Fmr1* gene [29]. ZFN pair s targeting the CATGAACAGTTTATCgtacgaGAAGATCTGATGGGT sequence in the *Fmr1* gene led to a 122 bp deletion that caused skipping of exon 8 and decreased Fmrp expression [72]. *Fmr1*-KO rats have been reported to display disrupted cort ical processing of auditory stimuli [30] and memory impairment based on hippoca mpal cellular and synaptic deficits [68]. For drug development in general, rat mod el can provide beneficial information to evaluate the safety risk of drug candidate s compared with mouse model since toxicity studies are usually conducted with ra ts. However, reports on other characteristics of *Fmr1*-KO rats remain limited.

In present study, I examined EEG phenotypes, such as basal EEG power and ASSR, in *Fmr1*-KO rats and conducted a brief behavioral assessment to examine its utility as an alternative preclinical model for drug development in FXS. ASSR is an electrophysiological response entrained to both frequency and phase of rapid, periodic acoustic stimuli [19, 73]. The entrainment is generally defined as two indices with time-frequency decomposition; ITC indicating phase consistency across trials and ERSP indicating event-related alteration of EEG frequency spectrum as a function of time. Accumulated evidence demonstrates the excellent test-retest reliability of ASSR in clinical setting, indicating the use of this method for drug development trial [3, 74-76]. I

employed the established methodology of ASSR with ERSP and ITC in rodent model (Fig. 1 in chapter I).

Materials and Methods

Animals

Five-week-old *Fmr1*-KO and WT rats were purchased from Oriental Yeast Co., Ltd. (Tokyo, Japan). *Fmr1*-KO rats were generated using the ZFN method [29], and the lines were first generated on an outbred Sprague-Dawley background at Sage Laboratories, LLC.

Surgery

Surgical operations were conducted in 13 WT and 14 *Fmr1*-KO male rats at 7–8 weeks of age to implant 4 electrodes under anesthesia with 2–2.5% isoflurane. A recording electrode was embedded onto the surface of the cortex using a customized switchable pedestal and electrode cables (S.E.R. Corporation, Tokyo, Japan). This paradigm using a switchable pedestal was previously developed to enable ECoG recordings to be taken from the parietal and temporal cortex in freely moving rats (Fig. 1 in chapter I). Briefly, the recording electrodes were placed at AP -1.0 mm/ML -1.0 mm (parietal cortex) and AP -4.5 mm/ML -7.5 mm/VD −4.0 mm (temporal cortex) relative to bregma. Reference and ground electrodes were placed at AP 8.0 mm/ML -1.5 mm and AP -10.0 mm/ML -1.5 mm, respectively. The switchable pedestal with stainless steel wire was attached to the cranium using methacrylic resin (GC Corporation, Tokyo, Japan). Rats were allowed to recover for approximately 14 days before testing. The rats were housed in groups until electrode implantation and then alone after implantation in ventilated cages under a 12-h light/dark cycle with food and water available *ad libitum*. All animal experimental procedures were performed in accordance with the Guide for the Care and Use of Laboratory Animals, 8th edition and approved by the Institutional Animal Care and Use

Committee of Astellas Pharma Inc. Furthermore, Astellas Pharma Inc., Tsukuba Research Center was awarded Accreditation Status by the AAALAC International.

Spontaneous locomotor activity

Locomotor activity was evaluated in rats implanted with a switchable pedestal at 9 weeks old. First, the rats were acclimated to the test room under 1 lux of red right. After 1 h of acclimation, test animals were moved from their home cages to new cages exposed to over 300 lux of light. Motor activity was measured for 90 min using a Supermex sensor (Muromachi inc., Tokyo, Japan) comprising paired infrared pyroelectric detectors that measure radiated body heat, and analyzed using CompACT AMS, ver. 3.82 (Muromachi Inc.). These data were divided into 3 time periods (0–30, 30–60, 60–90 min) and the total count was calculated for each time period.

EEG Recording

EEG experiments were performed according to established methods (General Fig. 1). Electrophysiological activity was recorded inside a Faraday cage with speakers attached to the top of the cage, using a high-impedance differential AC amplifier (model #1800, A-M Systems, Carlsbrog, WA, USA) and Spike 2 (CED, Cambridge, UK) with CED1401 (CED). All EEG experiments were performed in dim light (<300 lux). All animals were implanted with electrodes connected to an amplifier via electrode cables during habituation and recording, and were allowed to move freely. Data from Spike2 were converted using EEGLAB in the MATLAB toolbox (Math Works, Natick MA, USA). The EEG measurements were conducted at 10 weeks of age in all animals.

Measurement of power spectrum was conducted under a series of 200-paired white-noise stimuli presented 500 ms apart at 85 dB (10 ms in duration) with 9- to 13-s

randomized interstimulus intervals. Acoustic stimuli were presented using Spike 2 with CED 1401 for another experimental purpose. Single-trial epochs between -1 and 2 sec relative to the first click were extracted from continuous data. Analysis and calculations were performed using FFT analysis in the MATLAB toolbox. Absolute power was calculated at delta (0.5–4 Hz), theta (4–8 Hz), alpha (8–12 Hz), beta (12–30 Hz) and gamma (30–80 Hz) frequency bands in present study (General Fig. 2B). Relative values were calculated as the proportion of absolute power at each frequency band relative to total power (0–120 Hz).

For ASSR recording, auditory stimuli consisted of click sounds (80 dB) that included 500-msec trains at 10, 20, 30, 40, 50, 60, 70, and 80 Hz within a single train, as reported in previous study (General Fig. 1A). These stimuli were repeated 200 times/trial with an ITI and ISI of 600 msec. Each sound stimulus was generated using Spike2 with CED 1401. For analysis of ASSR, a low-pass filter (100 Hz) was applied to the EEG data to remove artifacts. The time-frequency decomposition during each click sound trains were calculated by wavelet transformation (frequency limit: 8 to 100 Hz, wavelet cycle: 10 to 62.5, epoch size: 9.0 sec). As output data, measurable factors were divided into two groups: ERSP (baseline: pre-stimulations from −600 to 0 msec) and ITC in the MATLAB toolbox (General Fig. 2A).

Statistics

Unpaired t-test was used to detect significant differences between *Fmr1*-KO and WT rats. Statistical analyses were conducted using GraphPad Prism, version 8.0.2 for Windows (GraphPad Software, San Diego CA, USA, http://www.graphpad.com). P values < 0.05 were considered statistically significant.

Results

Fmr1-KO rats display hyperactivity in a novel environment.

WT and *Fmr1*-KO rats displayed a time-dependent decrease in activity counts during the 90-min test period in novel cages (Fig. 1A). In the first 30 min, *Fmr1*-KO rats showed a significant increase in total activity counts compared with WT rats (Fig. 1B). In contrast, in the 30–60 min and 60–90 min time periods, total activity counts were not significantly different between *Fmr1*-KO rats and WT rats.

Fmr1-KO rats display enhanced gamma power.

Power spectrum analysis was calculated from basal power with no sound stimuli. Spectra of absolute power at around 40–80 Hz was higher in *Fmr1*-KO rats than in WT rats (Fig. 2A). Absolute power at the gamma frequency band (30–80 Hz) was significantly increased in *Fmr1*-KO rats compared with WT rats, while that at the alpha frequency band (8–12 Hz) tended to be decreased ($p=0.05$) (Fig. 2B). Relative power at the gamma frequency band was significantly increased in *Fmr1*-KO rats compared with WT rats (Fig. 2C). In contrast, relative power at alpha and beta frequency bands (12–30 Hz) was significantly decreased in *Fmr1*-KO rats. Absolute and relative power at delta (0.5–4 Hz) and theta frequency bands (4–8 Hz) were not significantly different between *Fmr1*-KO and WT rats.

Gamma synchronization of ITC and ERSP is reduced in *Fmr1*-KO rats.

ITC analysis showed that auditory click-train stimuli elicited frequency-dependent responses from 10 to 80 Hz in both *Fmr1*-KO and WT rats (Fig 3A). In the gamma frequency band (30–80 Hz) for ASSR, ITC reached a maximum at around 40–50 Hz in

both *Fmr1*-KO and WT rats (Fig 3B). ITC was significantly decreased at 30, 40, 50, 60, and 70 Hz in *Fmr1*-KO rats compared with WT rats. Meanwhile, there were no significant differences in ITC at 10, 20, 80 Hz between genotypes (Fig. 3C). In ERSP analysis, auditory click-train stimuli similarly elicited frequency-dependent responses in both *Fmr1*-KO and WT rats (Fig. 4A). *Fmr1*-KO rats showed lower ERSP than WT rats, although a peak response was observed at 40–50 Hz within the gamma frequency band in both *Fmr1*-KO and WT rats (Fig. 4B). ERSP was significantly decreased at 30, 40, 50, and 60 Hz in *Fmr1*-KO rats compared with WT rats. In contrast, there was no significant difference in ERSP at 10, 20, 70 and 80 Hz between *Fmr1*-KO and WT rats (Fig. 4C).

Discussion

While the behavioral and neurophysiological characterizations of *Fmr1* KO mice have been extensively replicated, those of *Fmr1*-KO rats remain limited. The present study is the first to describe the neurophysiological phenotypes of *Fmr1*-KO rats.

First, I assessed basal EEG profiles in *Fmr1*-KO rats. *Fmr1*-KO rats displayed significantly augmented basal gamma power compared to WT but decreased alpha power. This pattern of basal EEG power in *Fmr1*-KO rats is consistent with findings in subjects with FXS, who show augmented power in the gamma frequency band, but reduced power in the alpha frequency band [24, 61]. This augmented gamma power is also consistent with studies in *Fmr1* KO mice [71, 77], which display augmented neuronal excitability related to alterations in input to fast spiking inhibitory interneurons synchronized to the gamma frequency band [78, 79]. Alpha activity reportedly produces bouts of inhibition that repeat every 100 ms, and these alpha oscillations modulate gamma activity driven by GABAergic inhibitory activity in sensory information processing [80-82]. This pattern of increased gamma and decreased alpha power suggests the presence of impaired gamma activity with involvement from GABAergic neurons in *Fmr1*-KO rats. In this study, we did not observe any alterations in power in the theta frequency band, although power in the beta frequency band was reduced in *Fmr1*-KO rats. Subjects with FXS show enhanced basal theta power and no change in power in the beta frequency band [24, 61]. Resting power in the theta and beta frequency bands are not changed in *Fmr1* KO mice [71]. The discordance in theta and beta frequency bands between rodents and subjects with FXS is important to note and requires further study. Nevertheless, this finding that basal power is enhanced in the gamma frequency band in a preclinical rat model of FXS is consistent with the EEG phenotypes observed in *Fmr1* KO mice and subjects with FXS.

Enhanced neuronal excitability is associated with behavioral symptoms such as increased anxiety and locomotor activity [62, 83, 84], some of the most consistent behavioral symptoms observed in subjects with FXS [85]. The present study found that *Fmr1*-KO rats showed enhanced locomotor activity for the first 30 min after placement in a novel environment but not at 30–60 min or 60–90 min. Studies using *Fmr1* KO mice have reported that the hyperactivity was a reaction to novelty [86, 87]. The results from *Fmr1*-KO rats suggest that the hyperactivity may be a reaction to novelty, because the significant augmentation in locomotor activity was only observed for the first 30 min after placement in a novel testing field. Interestingly, startle response to sounds of collision between pedestal and top cage was observed in *Fmr1*-KO rats during measurement of locomotor activity only in *Fmr1*-KO not wild type rats (data not shown). Sensory hypersensitivity is a common phenotype in subjects with FXS [88], with habituation deficits to repeated sounds, especially N1 amplitude of ERP [22, 59, 60]. Further research of ERP responses and habituation to repeated sounds stimuli is needed. In vitro slice recordings have shown increased excitability in excitatory neurons from the somatosensory cortex of *Fmr1* KO mice [89]. Specific deletion of forebrain excitatory neurons in FMRP increases abnormal locomotor activity [31]. Taken together, these findings on basal power and hyperactivity suggest that *Fmr1*-KO rats exhibit cortical hyper-excitability as a pathophysiological consequence of FMRP deletion.

Second, I provide the first report of ASSR in *Fmr1*-KO rats. WT and *Fmr1*-KO rats showed clear ITC and ERSP responses at 10–80 Hz. Peak ITC and ERSP responses observed at 40–50 Hz in the gamma frequency band (30–80 Hz) are consistent with results in chapter I (Fig. 2 in chapter I) and humans [6, 43, 45]. ASSR recordings revealed clear impairment of ITC at 30–70 Hz in *Fmr1*-KO rats compared with WT rats. Additionally, *Fmr1*-KO rats demonstrated increased basal power in the gamma

frequency band. A similar impairment of the phase-locking factor of ASSR at only 30–58 Hz was observed in subjects with FXS, with phase-locking abnormalities reported to be associated with increased gamma single-trial power [5]. Further, there was also clear impairment of ERSP at 30–60 Hz in *Fmr1*-KO rats. I used a previously developed ASSR paradigm that adopted click sounds as stimuli in freely moving rats (General Fig. 2), with a similar methods having been used in subjects with schizophrenia [7]. However, no robust impairment of ERSP in the gamma frequency band has been observed in subjects with FXS or *Fmr1* KO mice. It is important to note that these studies used "chirp" stimuli to elicit ASSR [5, 71]. Although the differences associated with using "click" and "chirp" stimuli for eliciting ASSR remain elusive, the click auditory stimulus has been reported to induce large effect sizes and deficits in ASSR evoked by 40-Hz click stimulation have been used as a translational biomarker for schizophrenia [6, 90, 91]. These findings may support the use of click-stimuli-evoked ASSR as robust methods for determining ITC and ERSP in *Fmr1*-KO rats. Taken together, the specific attenuation of ASSR at 30–60 Hz in *Fmr1*-KO rats as it is in *Fmr1* KO mice and subjects with FXS suggests that ASSR in the gamma frequency band is a biomarker for FXS.

Fmr1-KO rats exhibited ASSR attenuation and enhanced basal power specific to gamma frequency band, these similar EEG features were observed in *Fmr1* KO mice and subjects with FXS [5, 24, 71]. Preclinical research in *Fmr1* KO mice has shown that increased gamma excitability decreases excitatory drive in fast-spiking inhibitory interneurons, resulting in increased and poorly synchronized pyramidal cell firing in the gamma frequency range [92]. *Fmr1*-KO rats show deficits of switching process from an elevated gamma state to a reduced gamma state with insufficiently synchronization related to firing rate of fast-spiking interneurons in visual cortex, and disrupted cortical processing of auditory stimuli [30, 93, 94]. These findings suggest that gamma power

abnormalities with gamma band-ASSR attenuation and augmented basal gamma power could attribute to imbalance between excitation and inhibition of the neural network in underlying mechanism of FXS.

Conclusions

The present study is the first report to investigate ASSR in a rat model of FXS along with locomotor activity and basal EEG power. *Fmr1*-KO rats displayed reduced basal EEG power at the alpha frequency band, enhanced power at the gamma frequency band, and hyperactivity, consistent with findings in subjects with FXS and *Fmr1* KO mice. Moreover, ASSR at 10–80 Hz peaked at 40 Hz and robust attenuation of ITC and ERSP was observed at 30–60 Hz in *Fmr1*-KO rats. ASSR at the gamma frequency band, along with abnormal basal EEG properties and hyperactivity, may be a translational biomarker across species. Taken together, these findings indicate that *Fmr1*-KO rats are a useful preclinical model of FXS, and will aid in the acceleration of drug development by testing drug candidates with synergistic gamma power analysis among various species [3, 77, 95].

Figures

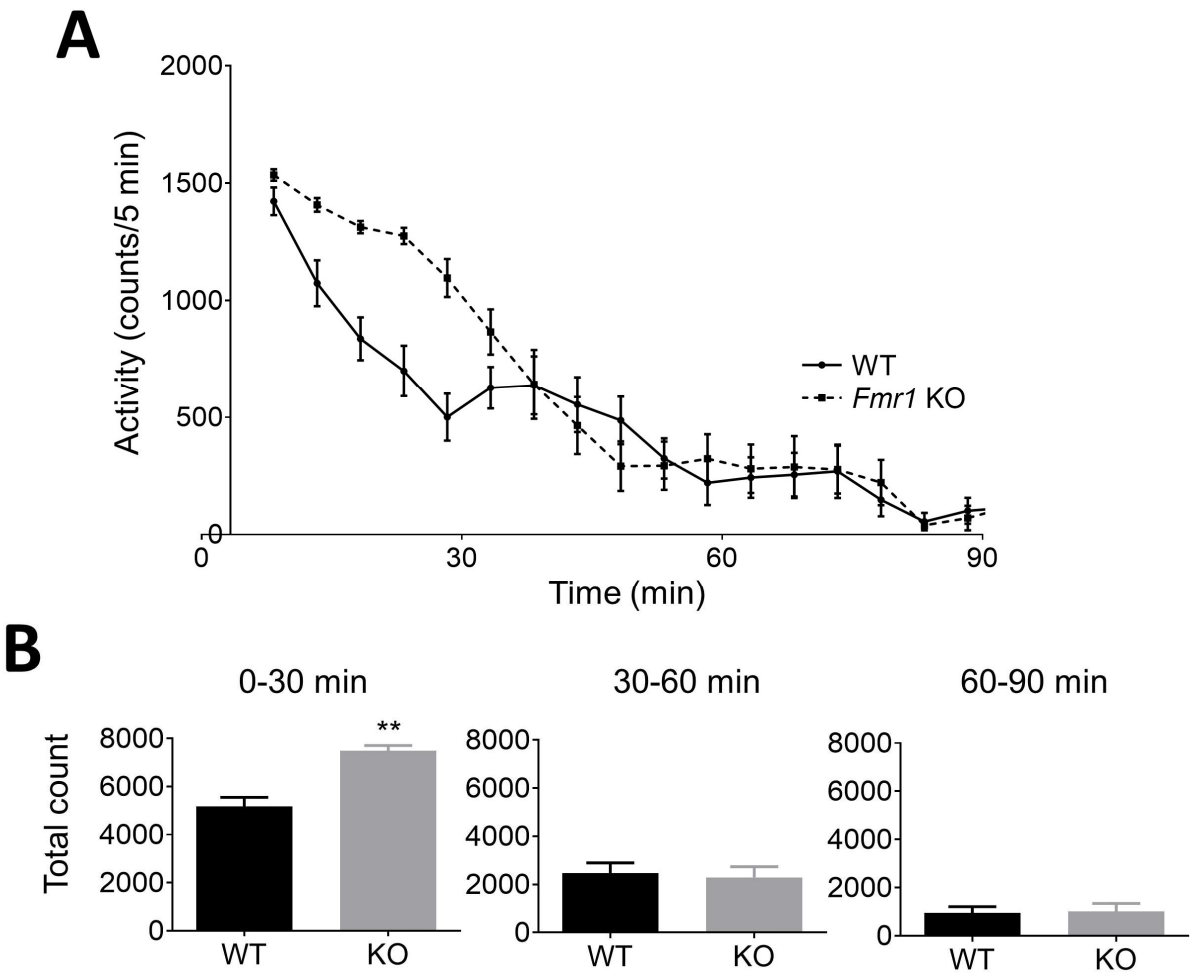

Fig. 1.

Fig. 1. Locomotor activity in *Fmr1*-KO and WT rats in a novel environment. (A) Time course of locomotor activity (counts/5 min) in WT (solid line) and *Fmr1*-KO rats (dashed line) across 90 min after placement in a novel cage. (B) Total activity counts at 3 time periods (0–30, 30–60, and 60–90 min) in WT and *Fmr1*-KO rats. Data represent mean ± SEM (n = 13–14). **P<0.01, significant differences between groups; unpaired t-test.

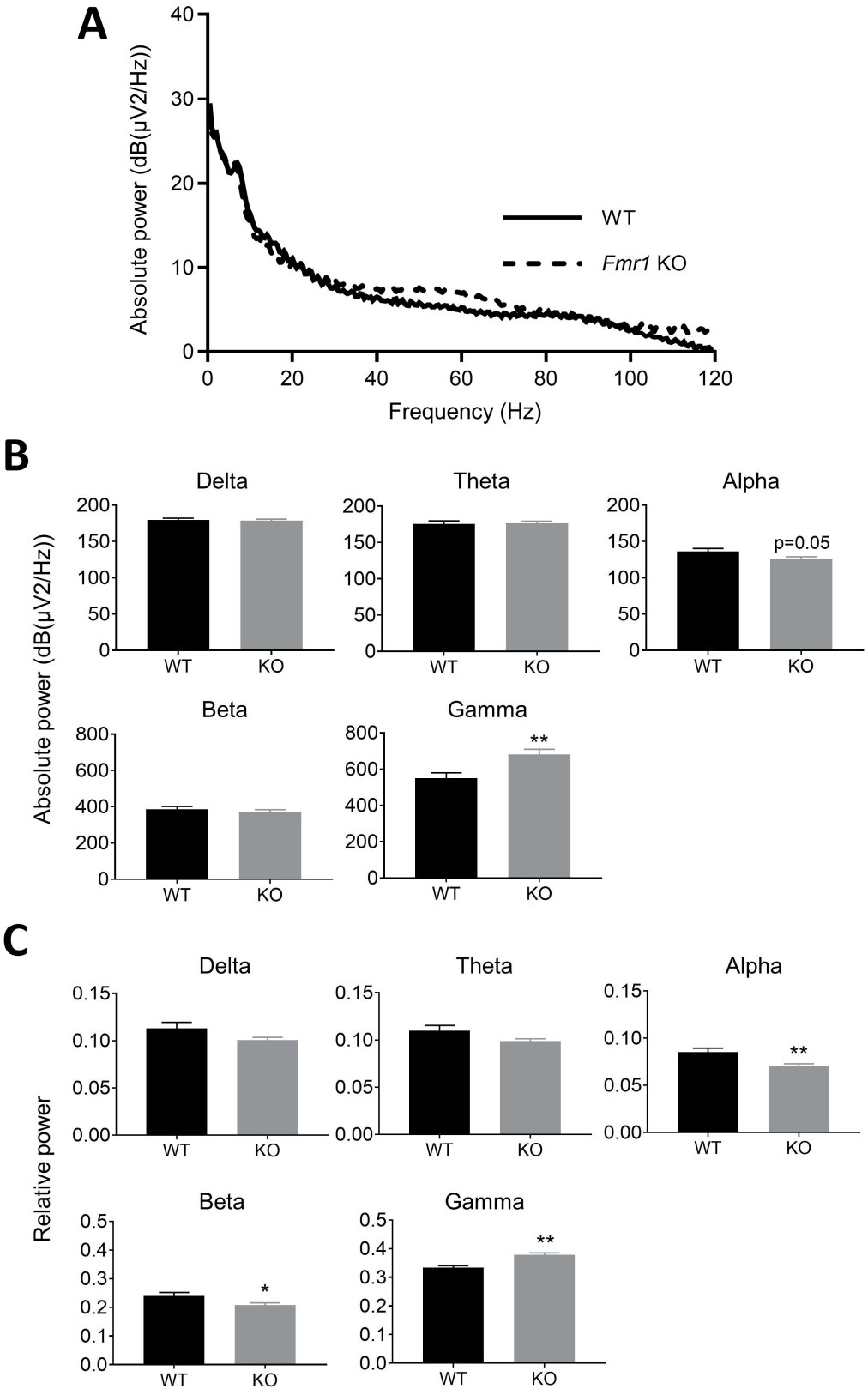
A
Absolute power (dB(μV2/Hz))
Frequency (Hz)
WT
Fmr1 KO
B
Absolute power (dB(μV2/Hz))
Delta
Theta
Alpha
p=0.05
Beta
Gamma
**
WT
KO
C
Relative power
Delta
Theta
Alpha
**
Beta
*
Gamma
**
WT
KO

Fig. 2.

Fig. 2. Comparison of basal power between *Fmr1*-KO and WT rats. (A) Spectra of basal absolute power between 0 and 120 Hz in WT (solid line) and *Fmr1*-KO rats (dashed line). (B) Absolute power at delta (0.5–4 Hz), theta (4–8 Hz), alpha (8–12 Hz), beta (12–30 Hz), and gamma (30–80 Hz) frequency bands in WT and *Fmr1*-KO rats. (C) Relative power at delta, theta, alpha, beta, and gamma frequency bands in WT and *Fmr1*-KO rats. Data represent mean ± SEM (n = 13–14). * $P<0.05$, ** $P<0.01$, significant differences between groups; unpaired t-test.

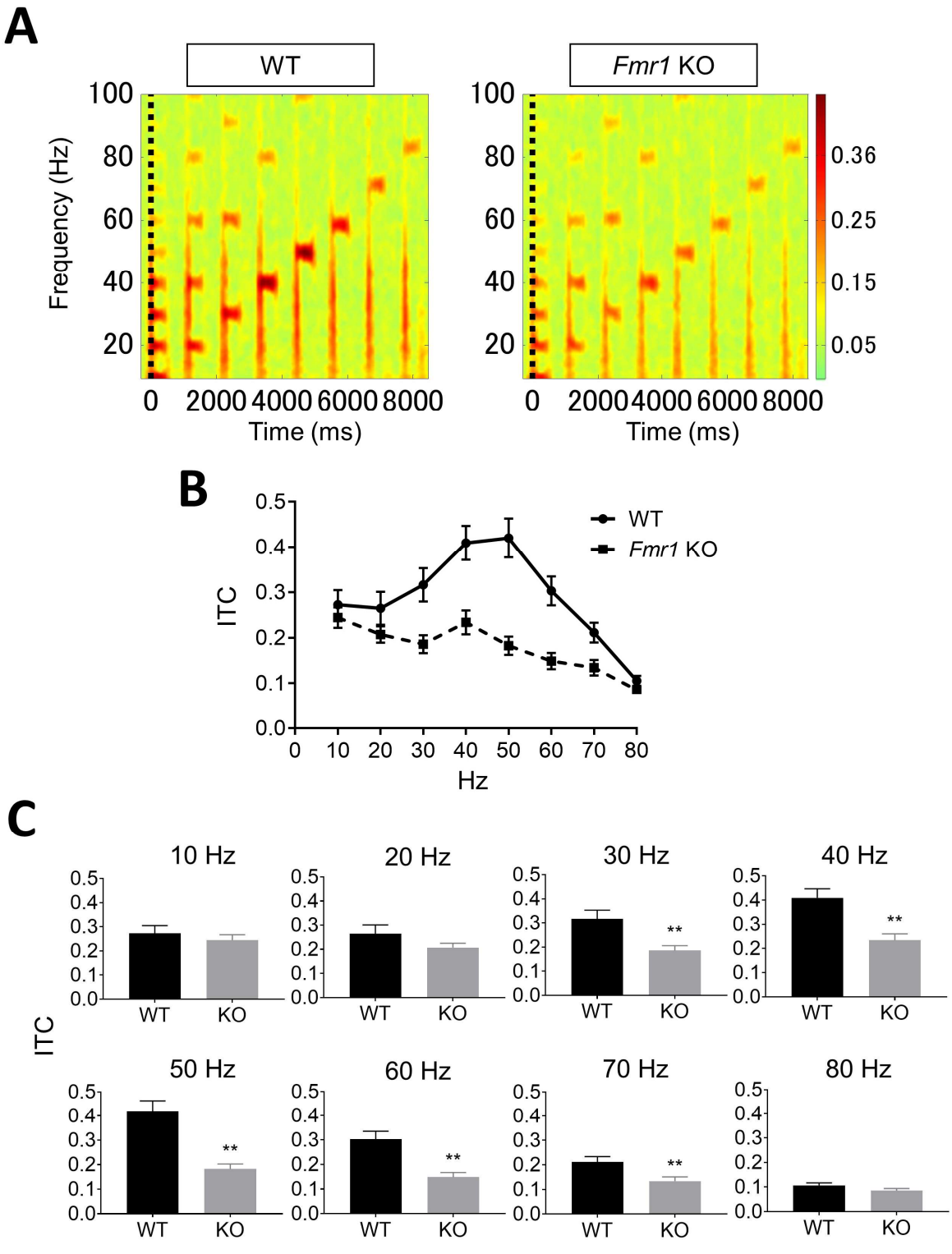
A
WT
Fmr1 KO
Frequency (Hz)
100
80
60
40
20
0
2000
4000
6000
8000
Time (ms)
0.36
0.25
0.15
0.05
B
ITC
Hz
WT
Fmr1 KO
C
10 Hz
20 Hz
30 Hz
40 Hz
50 Hz
60 Hz
70 Hz
80 Hz
WT
KO
**

Fig. 3.

Fig. 3. Comparison of inter-trial coherence (ITC) between *Fmr1*-KO and WT rats. (A) Time-frequency plots of ITC in WT and *Fmr1*-KO rats evoked by auditory click stimuli from 10 to 80 Hz. (B) Average of all ITC measured in WT (circle, solid line) and *Fmr1*-KO (square, dashed line) rats. (C) ITC in WT and *Fmr1*-KO rats at each frequency. Data represent mean ± SEM (n = 13–14). **P<0.01, significant differences between groups; unpaired t-test.

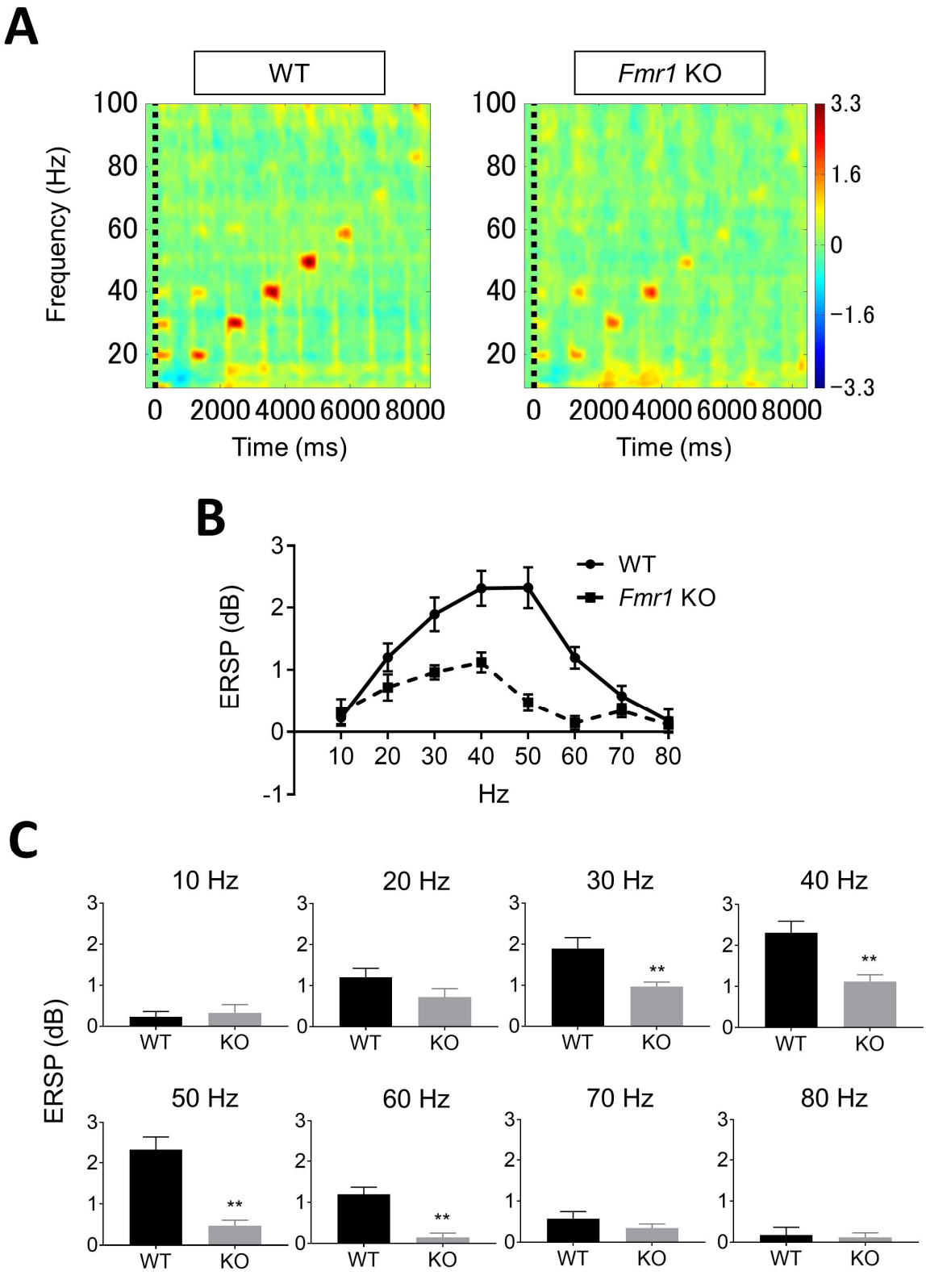
A
WT
Fmr1 KO
Frequency (Hz)
100
80
60
40
20
0
2000
4000
6000
8000
Time (ms)
3.3
1.6
0
−1.6
−3.3
B
ERSP (dB)
WT
Fmr1 KO
Hz
C
10 Hz
20 Hz
30 Hz
40 Hz
50 Hz
60 Hz
70 Hz
80 Hz
WT
KO
**

Fig. 4.

Fig. 4. Comparison of event-related spectral perturbation (ERSP) between *Fmr1*-KO and WT rats. (A) Time-frequency plots of ERSP in WT and *Fmr1*-KO rats evoked by auditory click stimuli from 10 to 80 Hz. (B) Average of all ERSP measured in WT (circle, solid line) and *Fmr1*-KO (square, dashed line) rats. (C) ERSP in WT and *Fmr1*-KO rats at each frequency. Data represent mean ± SEM (n = 13–14). **P<0.01, significant differences between groups; unpaired t-test.

General discussion

The present study showed gamma oscillatory responses of rats in two aspects with pharmacological response (chapter I) and genetic disease model (chapter II) to validate novel constructed methods for ASSR recording.

In the first chapter, the novel methods enabling for EEG to record at two brain regions of interest were constructed, which allows to compare the ASSR signals recorded at two brain regions between temporal and parietal cortex. Note that advantage for comparison of the EEG signals from multiple brain regions in same animal because the suitable recording region with potent response differs depending on the recording methods of EEG. The recording methods of ASSR to click stimuli with a wide frequency range enabled distinct detection of ERSP and ITC with each auditory click train stimulus, and the 40 Hz ASSR showed maximal ERSP and ITC, similar to humans. Ketamine exerted a bi-phasic effect on ASSR at gamma frequency bands (40–70 Hz) with increasing the basal power. In the second chapter, the EEG phenotypes were characterized in a recently established *Fmr1*-targeted transgenic rats to validate the constructed methods of ASSR. *Fmr1*-KO rats displayed robust attenuation of ITC and ERSP at gamma frequency bands (30–60 Hz), enhanced basal gamma power and hyperactivity, consistent with findings in subjects with FXS. These findings suggest that temporal cortex recording with a wide frequency range is a robust methodology to detect ASSR.

The development of new drugs encompasses a wide variety of topics, including the pharmacological profile (PK/PD, ADME, etc.) of each new drug and the ensuing response of the patient (ranging from cell- and molecular- changes to the amelioration of symptoms and changes in clinical endpoints) [3]. The bi-phasic effect of ASSR at gamma bands with increasing the basal gamma power was observed by administration of ketamine in the chapter I. The ketamine at 30 mg/kg induced a biphasic effect on PLF of 40 Hz ASSR based on the PK/PD response [16]. Yamazaki et al. in our groups successfully detected

dose and time-dependent effects of GABAa receptor antagonist in ASSR signals with increasing in basal gamma power [95]. These findings suggested that studies using ASSR and basal gamma power following administration of an investigational drug are technically suited to capture dosing levels to corroborate PK/PD data. This recording system using ASSR and basal gamma power may be enabled to valuable retrospective information on dosing levels and therapeutic windows to act as a useful secondary biomarker of efficacy and receptor occupancy to corroborate PK/PD data in the future [96, 97].

The repeated failures of new investigational drugs for neuropsychiatric disorders also emphasize the need for new drug discovery approaches that target specific pathophysiological alterations shared in pre-stratified patient populations [3, 4]. The abnormality of ASSR at gamma bands in *Fmr1*-targeted transgenic rat model of fragile X syndrome was observed in the chapter II, which is consistent with the patients with FXS. These results suggest that ASSR abnormalities are a translatable biomarker over the species and demonstrate the utility for investigating drugs for the treatment of FXS. Numerous studies have suggested that alterations in gamma oscillation likely reflect the activity of PV positive GABAergic interneuron populations which plays an important role in sensory input and processing [25, 26]. Indeed, forebrain excitatory neuron selective deletion of the *fmr1* gene leads to reduction of density of PV cells and enhancement of basal EEG gamma power [31]. GABAa receptor antagonist results in the dose-dependently reduced ASSR signals with increased baseline gamma power of rats in same recording methods [95]. The NMDAR antagonist, ketamine showed bi-phasic effect of ASSR specific to gamma frequency bands in the chapter I. The blunting NMDA signaling transduction in PV positive interneurons increases basal gamma power, while decreases evoked gamma power [26, 27]. From these findings, the consistent appearance of altered

ASSR gamma power is both widespread across species and in support of the interneuron-mediated E/I imbalance theory. The ASSR disruptions at gamma in the present study are caused by augmented basal gamma activity. In this case, an increase in baseline gamma levels—presumably a product of the inhibition of the GABA interneurons—decreases the signal-to-noise ratio and reduces evoked gamma in the absence of any change in peak response. The use of ASSR gamma power for biomarker-based stratification may be useful for neuropsychiatric disorders that display altered evoked gamma such as FXS [5, 66], schizophrenia [6, 7, 90, 91], bipolar disorder [20, 98-102], autism [103, 104], and 22q11.2 deletion [105]. For these diseases, incorporation of a prospective screen would aid in the selection of a more appropriate trial population and, in the case of ineffective compounds, possibly reveal a candidate's lack of efficacy at an earlier stage.

In conclusion, the present study demonstrated that ASSR gamma power signals can be well recorded with the constructed recording methods in rodents, which allows us to study pharmacological responses and disease phenotype as observed in human. These findings suggest the ASSR gamma power signals are promising biomarker and the constructed recording methods are tool for bridging to subjects with neuropsychiatric disorders from rodents. Further study with this system will uncover the more detail mechanism of ASSR, potentially enabling to investigate new drugs for neuropsychiatric disorders as a translational biomarker.

Acknowledgements

This work was based on the official research contract between Astellas Pharma Inc.

I am deeply grateful to Drs. Sokichi Honda, Ai Okamura, Takuma Mihara, Mitsuyuki Matsumoto, Takatoshi Soga in Astellas Pharma Inc., for helpful technical supports, insightful discussions and encouragement.

I am grateful to Prof. Kiyoto Kasai, Research Associate Mariko Tada, Associate Prof. Kenji Kirihara, Dr. Zhilei Zhao, Associate Prof. Seiichiro Jinde, Prof. Takanori Uka for intellectual input of recording methods and interpretation of data based on the official research contract between Astellas Pharma Inc. and the University of Tokyo.

I am grateful to Dr. Hiroshi Yamada in Otsuka Pharma Inc., for intellectual input of recording methods and interpretation of data.

Finally, I would like to appreciate my family for their continuous encouragement and support.

References

1 Erickson CA, Davenport MH, Schaefer TL, Wink LK, Pedapati EV, Sweeney JA, Fitzpatrick SE, Brown WT, Budimirovic D, Hagerman RJ, Hessl D, Kaufmann WE, Berry-Kravis E: Fragile x targeted pharmacotherapy: Lessons learned and future directions. Journal of Neurodevelopmental Disorders 2017;9:7.

2 Beck K, Javitt DC, Howes OD: Targeting glutamate to treat schizophrenia: Lessons from recent clinical studies. Psychopharmacology 2016;233:2425-2428.

3 Honda S, Matsumoto M, Tajinda K, Mihara T: Enhancing clinical trials through synergistic gamma power analysis. Frontiers in Psychiatry 2020;11:537-537.

4 Matsumoto M, Walton NM, Yamada H, Kondo Y, Marek GJ, Tajinda K: The impact of genetics on future drug discovery in schizophrenia. Expert Opinion on Drug Discovery 2017;12:673-686.

5 Ethridge LE, White SP, Mosconi MW, Wang J, Pedapati EV, Erickson CA, Byerly MJ, Sweeney JA: Neural synchronization deficits linked to cortical hyper-excitability and auditory hypersensitivity in fragile x syndrome. Molecular Autism 2017;8:22.

6 O'Donnell BF, Vohs JL, Krishnan GP, Rass O, Hetrick WP, Morzorati SL: The auditory steady-state response (assr): A translational biomarker for schizophrenia. Supplements to Clinical neurophysiology 2013;62:101-112.

7 Tada M, Nagai T, Kirihara K, Koike S, Suga M, Araki T, Kobayashi T, Kasai K: Differential alterations of auditory gamma oscillatory responses between pre-onset high-risk individuals and first-episode schizophrenia. Cerebral Cortex 2016;26:1027-1035.

8 Korostenskaja M, Ruksenas O, Pipinis E, Griskova-Bulanova I: Phase-locking index and power of 40-hz auditory steady-state response are not related to major personality trait dimensions. Experimental Brain Research 2016;234:711-719.

9 Kuriki S, Kobayashi Y, Kobayashi T, Tanaka K, Uchikawa Y: Steady-state meg responses elicited by a sequence of amplitude-modulated short tones of different carrier frequencies. Hearing Research 2013;296:25-35.

10 Spencer KM, Niznikiewicz MA, Nestor PG, Shenton ME, McCarley RW: Left auditory cortex gamma synchronization and auditory hallucination symptoms in schizophrenia. BMC Neuroscience 2009;10:85.

11 Poulsen C, Picton TW, Paus T: Age-related changes in transient and oscillatory brain responses to auditory stimulation in healthy adults 19-45 years old. Cerebral Cortex 2007;17:1454-1467.

12 Farahani ED, Goossens T, Wouters J, van Wieringen A: Spatiotemporal reconstruction of auditory steady-state responses to acoustic amplitude modulations: Potential sources beyond the auditory pathway. NeuroImage 2017;148:240-253.

13 Spencer KM: Baseline gamma power during auditory steady-state stimulation in schizophrenia. Frontiers in Human Neuroscience 2011;5:190.

14 Mulert C, Kirsch V, Pascual-Marqui R, McCarley RW, Spencer KM: Long-range synchrony of gamma oscillations and auditory hallucination symptoms in schizophrenia. International Journal of

Psychophysiology 2011;79:55-63.
15 Reyes SA, Lockwood AH, Salvi RJ, Coad ML, Wack DS, Burkard RF: Mapping the 40-hz auditory steady-state response using current density reconstructions. Hearing Research 2005;204:1-15.
16 Sivarao DV, Chen P, Senapati A, Yang Y, Fernandes A, Benitex Y, Whiterock V, Li YW, Ahlijanian MK: 40 hz auditory steady-state response is a pharmacodynamic biomarker for cortical nmda receptors. Neuropsychopharmacology 2016;41:2232-2240.
17 Zhang J, Ma L, Li W, Yang P, Qin L: Cholinergic modulation of auditory steady-state response in the auditory cortex of the freely moving rat. Neuroscience 2016;324:29-39.
18 Sivarao DV, Frenkel M, Chen P, Healy FL, Lodge NJ, Zaczek R: Mk-801 disrupts and nicotine augments 40 hz auditory steady state responses in the auditory cortex of the urethane-anesthetized rat. Neuropharmacology 2013;73:1-9.
19 Brenner CA, Krishnan GP, Vohs JL, Ahn WY, Hetrick WP, Morzorati SL, O'Donnell BF: Steady state responses: Electrophysiological assessment of sensory function in schizophrenia. Schizophrenia Bulletin 2009;35:1065-1077.
20 Spencer KM, Salisbury DF, Shenton ME, McCarley RW: Gamma-band auditory steady-state responses are impaired in first episode psychosis. Biological Psychiatry 2008;64:369-375.
21 Light GA, Hsu JL, Hsieh MH, Meyer-Gomes K, Sprock J, Swerdlow NR, Braff DL: Gamma band oscillations reveal neural network cortical coherence dysfunction in schizophrenia patients. Biological Psychiatry 2006;60:1231-1240.
22 Ethridge LE, White SP, Mosconi MW, Wang J, Byerly MJ, Sweeney JA: Reduced habituation of auditory evoked potentials indicate cortical hyper-excitability in fragile x syndrome. Translational Psychiatry 2016;6:e787.
23 Verkerk AJMH, Pieretti M, Sutcliffe JS, Fu YH, Kuhl DPA, Pizzuti A, Reiner O, Richards S, Victoria MF, Zhang F, Eussen BE, van Ommen GJB, Blonden LAJ, Riggins GJ, Chastain JL, Kunst CB, Galjaard H, Thomas Caskey C, Nelson DL, Oostra BA, Warren ST: Identification of a gene (fmr-1) containing a cgg repeat coincident with a breakpoint cluster region exhibiting length variation in fragile x syndrome. Cell 1991;65:905-914.
24 Wang J, Ethridge LE, Mosconi MW, White SP, Binder DK, Pedapati EV, Erickson CA, Byerly MJ, Sweeney JA: A resting eeg study of neocortical hyperexcitability and altered functional connectivity in fragile x syndrome. Journal of Neurodevelopmental Disorders 2017;9:11.
25 Lewis DA, Curley AA, Glausier JR, Volk DW: Cortical parvalbumin interneurons and cognitive dysfunction in schizophrenia. Trends in neurosciences 2012;35:57-67.
26 Carlen M, Meletis K, Siegle JH, Cardin JA, Futai K, Vierling-Claassen D, Ruhlmann C, Jones SR, Deisseroth K, Sheng M, Moore CI, Tsai LH: A critical role for nmda receptors in parvalbumin interneurons for gamma rhythm induction and behavior. Molecular Psychiatry 2012;17:537-548.
27 Gandal MJ, Sisti J, Klook K, Ortinski PI, Leitman V, Liang Y, Thieu T, Anderson R, Pierce RC, Jonak G, Gur RE, Carlson G, Siegel SJ: Gabab-mediated rescue of altered excitatory-inhibitory balance, gamma synchrony and behavioral deficits following constitutive nmdar-hypofunction. Translational

Psychiatry 2012;2:e142.
28 Wang M, Arnsten AFT: Contribution of nmda receptors to dorsolateral prefrontal cortical networks in primates. Neuroscience Bulletin 2015;31:191-197.
29 Hamilton SM, Green JR, Veeraragavan S, Yuva L, McCoy A, Wu Y, Warren J, Little L, Ji D, Cui X, Weinstein E, Paylor R: Fmr1 and nlgn3 knockout rats: Novel tools for investigating autism spectrum disorders. Behavioral Neuroscience 2014;128:103-109.
30 Engineer CT, Centanni TM, Im KW, Rahebi KC, Buell EP, Kilgard MP: Degraded speech sound processing in a rat model of fragile x syndrome. Brain Research 2014;1564:72-84.
31 Lovelace JW, Rais M, Palacios AR, Shuai XS, Bishay S, Popa O, Pirbhoy PS, Binder DK, Nelson DL, Ethell IM, Razak KA: Deletion of fmr1 from forebrain excitatory neurons triggers abnormal cellular, eeg, and behavioral phenotypes in the auditory cortex of a mouse model of fragile x syndrome. Cerebral Cortex 2019;30:969-988.
32 Luts H, Desloovere C, Wouters J: Clinical application of dichotic multiple-stimulus auditory steady-state responses in high-risk newborns and young children. Audiology and Neurotology 2006;11:24-37.
33 Picton TW, John MS, Dimitrijevic A, Purcell D: Human auditory steady-state responses: Respuestas auditivas de estado estable en humanos. International Journal of Audiology 2003;42:177-219.
34 Herdman AT, Lins O, Van Roon P, Stapells DR, Scherg M, Picton TW: Intracerebral sources of human auditory steady-state responses. Brain Topography 2002;15:69-86.
35 Griskova-Bulanova I, Dapsys K, Maciulis V, Arnfred SM: Closed eyes condition increases auditory brain responses in schizophrenia. Psychiatry Research: Neuroimaging 2012;211:183-185.
36 Griskova-Bulanova I, Ruksenas O, Dapsys K, Maciulis V, Arnfred SM: Distraction task rather than focal attention modulates gamma activity associated with auditory steady-state responses (assrs). Clinical Neurophysiology 2011;122:1541-1548.
37 Vohs JL, Chambers RA, O'Donnell BF, Krishnan GP, Morzorati SL: Auditory steady state responses in a schizophrenia rat model probed by excitatory/inhibitory receptor manipulation. International Journal of Psychophysiology 2012;86:136-142.
38 van den Broek SP, Reinders F, Donderwinkel M, Peters MJ: Volume conduction effects in eeg and meg. Electroencephalography and Clinical Neurophysiology 1998;106:522-534.
39 Wang Y, Ma L, Wang X, Qin L: Differential modulation of the auditory steady state response and inhibitory gating by chloral hydrate anesthesia. Scientific Reports 2018;8:3683.
40 Saunders JA, Gandal MJ, Roberts TP, Siegel SJ: Nmda antagonist mk801 recreates auditory electrophysiology disruption present in autism and other neurodevelopmental disorders. Behavioural Brain Research 2012;234:233-237.
41 Umbricht D, Schmid L, Koller R, Vollenweider FX, Hell D, Javitt DC: Ketamine-induced deficits in auditory and visual context-dependent processing in healthy volunteers: Implications for models of cognitive deficits in schizophrenia. Archives of General Psychiatry 2000;57:1139-1147.
42 Sullivan EM, Timi P, Hong LE, O'Donnell P: Effects of nmda and gaba-a receptor antagonism on

auditory steady-state synchronization in awake behaving rats. International Journal of Neuropsychopharmacology 2015;18:pyu118.

43 Artieda J, Valencia M, Alegre M, Olaziregi O, Urrestarazu E, Iriarte J: Potentials evoked by chirp-modulated tones: A new technique to evaluate oscillatory activity in the auditory pathway. Clinical Neurophysiology 2004;115:699-709.

44 Cho RY, Konecky RO, Carter CS: Impairments in frontal cortical γ synchrony and cognitive control in schizophrenia. Proceedings of the National Academy of Sciences 2006;103:19878-19883.

45 Puvvada KC, Summerfelt A, Du X, Krishna N, Kochunov P, Rowland LM, Simon JZ, Hong LE: Delta vs gamma auditory steady state synchrony in schizophrenia. Schizophrenia Bulletin 2018;44:378-387.

46 Perez-Alcazar M, Nicolas MJ, Valencia M, Alegre M, Lopez-Azcarate J, Iriarte J, Artieda J: Cortical oscillations scan using chirp-evoked potentials in 6-hydroxydopamine rat model of parkinson's disease. Brain Research 2010;1310:58-67.

47 Wilding TS, McKay CM, Baker RJ, Kluk K: Auditory steady state responses in normal-hearing and hearing-impaired adults: An analysis of between-session amplitude and latency repeatability, test time, and f ratio detection paradigms. Ear and Hearing 2012;33:267-278.

48 Roopun AK, Cunningham MO, Racca C, Alter K, Traub RD, Whittington MA: Region-specific changes in gamma and beta2 rhythms in nmda receptor dysfunction models of schizophrenia. Schizophrenia Bulletin 2008;34:962-973.

49 Hashimoto T, Volk DW, Eggan SM, Mirnics K, Pierri JN, Sun Z, Sampson AR, Lewis DA: Gene expression deficits in a subclass of gaba neurons in the prefrontal cortex of subjects with schizophrenia. The Journal of Neuroscience 2003;23:6315-6326.

50 Plourde G, Baribeau J, Bonhomme V: Ketamine increases the amplitude of the 40-hz auditory steady-state response in humans. British Journal of Anaesthesia 1997;78:524-529.

51 Vlisides PE, Bel-Bahar T, Lee U, Li D, Kim H, Janke E, Tarnal V, Pichurko AB, McKinney AM, Kunkler BS, Picton P, Mashour GA: Neurophysiologic correlates of ketamine sedation and anesthesia: A high-density electroencephalography study in healthy volunteers. Anesthesiology 2017;127:58-69.

52 Hiyoshi T, Kambe D, Karasawa J, Chaki S: Differential effects of nmda receptor antagonists at lower and higher doses on basal gamma band oscillation power in rat cortical electroencephalograms. Neuropharmacology 2014;85:384-396.

53 NIMH: The national institute of mental health strategic plan; the bipolar schizophrenia network on intermediate phenotypes, The National Institute of Mental Health, 2008.

54 Javitt D, Keefe R, Walling DP, Ereshefsky L: Erp biomarker qualification consortium, 2019.

55 Okabe T, Matsuda T, Ohtsuka T, Watanabe M, Okano H, Miyawaki A: Brain mapping by integrated neurotechnologies for disease studies project, 2013.

56 Turner G, Webb T, Wake S, Robinson H: Prevalence of fragile x syndrome. American Journal of Medical Genetics 1996;64:196-197.

57 Lee AW, Ventola P, Budimirovic D, Berry-Kravis E, Visootsak J: Clinical development of

targeted fragile x syndrome treatments: An industry perspective. Brain sciences 2018;8:214.
58 Hagerman RJ, Berry-Kravis E, Hazlett HC, Bailey DB, Jr., Moine H, Kooy RF, Tassone F, Gantois I, Sonenberg N, Mandel JL, Hagerman PJ: Fragile x syndrome. Nature Reviews Disease Primers 2017;3:17065.
59 Castrén M, Pääkkönen A, Tarkka IM, Ryynänen M, Partanen J: Augmentation of auditory n1 in children with fragile x syndrome. Brain Topography 2003;15:165-171.
60 Schneider A, Leigh MJ, Adams P, Nanakul R, Chechi T, Olichney J, Hagerman R, Hessl D: Electrocortical changes associated with minocycline treatment in fragile x syndrome. Journal of Psychopharmacology 2013;27:956-963.
61 Van der Molen MJ, Van der Molen MW: Reduced alpha and exaggerated theta power during the resting-state eeg in fragile x syndrome. Biological Psychiatry 2013;92:216-219.
62 Ciaccio C, Fontana L, Milani D, Tabano S, Miozzo M, Esposito S: Fragile x syndrome: A review of clinical and molecular diagnoses. Italian Journal of Pediatrics 2017;43:39.
63 Knoth IS, Vannasing P, Major P, Michaud JL, Lippe S: Alterations of visual and auditory evoked potentials in fragile x syndrome. International Journal of Developmental Neuroscience 2014;36:90-97.
64 Van der Molen MJ, Van der Molen MW, Ridderinkhof KR, Hamel BC, Curfs LM, Ramakers GJ: Auditory and visual cortical activity during selective attention in fragile x syndrome: A cascade of processing deficiencies. Clinical Neurophysiology 2012;123:720-729.
65 Van der Molen MJ, Van der Molen MW, Ridderinkhof KR, Hamel BC, Curfs LM, Ramakers GJ: Auditory change detection in fragile x syndrome males: A brain potential study. Clinical Neurophysiology 2012;123:1309-1318.
66 Ethridge LE, De Stefano LA, Schmitt LM, Woodruff NE, Brown KL, Tran M, Wang J, Pedapati EV, Erickson CA, Sweeney JA: Auditory eeg biomarkers in fragile x syndrome: Clinical relevance. Frontiers in Integrative Neuroscience 2019;13:60.
67 Dahlhaus R: Of men and mice: Modeling the fragile x syndrome. Frontiers in Molecular Neuroscience 2018;11:41.
68 Till SM, Asiminas A, Jackson AD, Katsanevaki D, Barnes SA, Osterweil EK, Bear MF, Chattarji S, Wood ER, Wyllie DJ, Kind PC: Conserved hippocampal cellular pathophysiology but distinct behavioural deficits in a new rat model of fxs. Human Molecular Genetics 2015;24:5977-5984.
69 Grossman AW, Elisseou NM, McKinney BC, Greenough WT: Hippocampal pyramidal cells in adult fmr1 knockout mice exhibit an immature-appearing profile of dendritic spines. Brain Research 2006;1084:158-164.
70 Kazdoba TM, Leach PT, Silverman JL, Crawley JN: Modeling fragile x syndrome in the fmr1 knockout mouse. Intractable & rare diseases research 2014;3:118-133.
71 Lovelace JW, Ethell IM, Binder DK, Razak KA: Translation-relevant eeg phenotypes in a mouse model of fragile x syndrome. Neurobiology of Disease 2018;115:39-48.
72 Golden CEM, Breen MS, Koro L, Sonar S, Niblo K, Browne A, Burlant N, Di Marino D, De Rubeis S, Baxter MG, Buxbaum JD, Harony-Nicolas H: Deletion of the kh1 domain of fmr1 leads to

transcriptional alterations and attentional deficits in rats. Cerebral Cortex 2019;29:2228-2244.
73 Galambos R, Makeig S, Talmachoff PJ: A 40-hz auditory potential recorded from the human scalp. Proceedings of the National Academy of Sciences 1981;78:2643-2647.
74 Roach BJ, D'Souza DC, Ford JM, Mathalon DH: Test-retest reliability of time-frequency measures of auditory steady-state responses in patients with schizophrenia and healthy controls. NeuroImage: Clinical 2019;23:101878.
75 Legget KT, Hild AK, Steinmetz SE, Simon ST, Rojas DC: Meg and eeg demonstrate similar test-retest reliability of the 40 hz auditory steady-state response. International Journal of Psychophysiology 2017;114:16-23.
76 McFadden KL, Steinmetz SE, Carroll AM, Simon ST, Wallace A, Rojas DC: Test-retest reliability of the 40 hz eeg auditory steady-state response. PLoS One 2014;9:e85748.
77 Sinclair D, Featherstone R, Naschek M, Nam J, Du A, Wright S, Pance K, Melnychenko O, Weger R, Akuzawa S, Matsumoto M, Siegel SJ: Gaba-b agonist baclofen normalizes auditory-evoked neural oscillations and behavioral deficits in the fmr1 knockout mouse model of fragile x syndrome. eNeuro 2017;4:ENEURO.0380-0316.2017.
78 Cea-Del Rio CA, Huntsman MM: The contribution of inhibitory interneurons to circuit dysfunction in fragile x syndrome. Frontiers in Cellular Neuroscience 2014;8:245.
79 Salkoff DB, Zagha E, Yuzgec O, McCormick DA: Synaptic mechanisms of tight spike synchrony at gamma frequency in cerebral cortex. Journal of Neuroscience 2015;35:10236-10251.
80 Jensen O, Mazaheri A: Shaping functional architecture by oscillatory alpha activity: Gating by inhibition. Frontiers in Human Neuroscience 2010;4:186.
81 Mathewson KE, Lleras A, Beck DM, Fabiani M, Ro T, Gratton G: Pulsed out of awareness: Eeg alpha oscillations represent a pulsed-inhibition of ongoing cortical processing. Frontiers in Psychology 2011;2:99.
82 Mazaheri A, Jensen O: Rhythmic pulsing: Linking ongoing brain activity with evoked responses. Frontiers in Human Neuroscience 2010;4:177.
83 Braat S, Kooy RF: The gabaa receptor as a therapeutic target for neurodevelopmental disorders. Neuron 2015;86:1119-1130.
84 Penagarikano O, Mulle JG, Warren ST: The pathophysiology of fragile x syndrome. Annual review of genomics and human genetics 2007;8:109-129.
85 Tranfaglia MR: The psychiatric presentation of fragile x: Evolution of the diagnosis and treatment of the psychiatric comorbidities of fragile x syndrome. Developmental Neuroscience 2011;33:337-348.
86 Carreno-Munoz MI, Martins F, Medrano MC, Aloisi E, Pietropaolo S, Dechaud C, Subashi E, Bony G, Ginger M, Moujahid A, Frick A, Leinekugel X: Potential involvement of impaired bkca channel function in sensory defensiveness and some behavioral disturbances induced by unfamiliar environment in a mouse model of fragile x syndrome. Neuropsychopharmacology 2018;43:492-502.
87 Kramvis I, Mansvelder HD, Loos M, Meredith R: Hyperactivity, perseveration and increased

responding during attentional rule acquisition in the fragile x mouse model. Frontiers in Behavioral Neuroscience 2013;7:172.

88 Tsiouris JA, Brown WT: Neuropsychiatric symptoms of fragile x syndrome. CNS Drugs 2004;18:687-703.

89 Hays SA, Huber KM, Gibson JR: Altered neocortical rhythmic activity states in fmr1 ko mice are due to enhanced mglur5 signaling and involve changes in excitatory circuitry. Journal of Neuroscience 2011;31:14223-14234.

90 Griskova-Bulanova I, Dapsys K, Melynyte S, Voicikas A, Maciulis V, Andruskevicius S, Korostenskaja M: 40hz auditory steady-state response in schizophrenia: Sensitivity to stimulation type (clicks versus flutter amplitude-modulated tones). Neuroscience Letters 2018;662:152-157.

91 Thune H, Recasens M, Uhlhaas PJ: The 40-hz auditory steady-state response in patients with schizophrenia: A meta-analysis. JAMA Psychiatry 2016;73:1145-1153.

92 Gibson JR, Bartley AF, Hays SA, Huber KM: Imbalance of neocortical excitation and inhibition and altered up states reflect network hyperexcitability in the mouse model of fragile x syndrome. Journal of Neurophysiology 2008;100:2615-2626.

93 Berzhanskaya J, Phillips MA, Gorin A, Lai C, Shen J, Colonnese MT: Disrupted cortical state regulation in a rat model of fragile x syndrome. Cerebral Cortex 2017;27:1386-1400.

94 Berzhanskaya J, Phillips MA, Shen J, Colonnese MT: Sensory hypo-excitability in a rat model of fetal development in fragile x syndrome. Scientific Reports 2016;6:30769.

95 Yamazaki M, Honda S, Tamaki K, Irie M, Mihara T: Effects of (+)-bicuculline, a gabaa receptor antagonist, on auditory steady state response in free-moving rats. PLoS One 2020;15:e0236363.

96 Sanacora G, Smith MA, Pathak S, Su HL, Boeijinga PH, McCarthy DJ, Quirk MC: Lanicemine: A low-trapping nmda channel blocker produces sustained antidepressant efficacy with minimal psychotomimetic adverse effects. Molecular Psychiatry 2014;19:978-985.

97 Agbo F, Bui KH, Zhou D: Population pharmacokinetic analysis of lanicemine (azd6765), an nmda channel blocker, in healthy subjects and patients with major depressive disorder. Journal of Clinical Pharmacy and Therapeutics 2017;42:539-546.

98 O'Donnell BF, Hetrick WP, Vohs JL, Krishnan GP, Carroll CA, Shekhar A: Neural synchronization deficits to auditory stimulation in bipolar disorder. NeuroReport 2004;15:1369-1372.

99 Isomura S, Onitsuka T, Tsuchimoto R, Nakamura I, Hirano S, Oda Y, Oribe N, Hirano Y, Ueno T, Kanba S: Differentiation between major depressive disorder and bipolar disorder by auditory steady-state responses. Journal of Affective Disorders 2016;190:800-806.

100 Oda Y, Onitsuka T, Tsuchimoto R, Hirano S, Oribe N, Ueno T, Hirano Y, Nakamura I, Miura T, Kanba S: Gamma band neural synchronization deficits for auditory steady state responses in bipolar disorder patients. PloS One 2012;7:e39955.

101 Rass O, Krishnan G, Brenner CA, Hetrick WP, Merrill CC, Shekhar A, O'Donnell BF: Auditory steady state response in bipolar disorder: Relation to clinical state, cognitive performance, medication status, and substance disorders. Bipolar Disord 2010;12:793-803.

102 Reite M, Teale P, Rojas DC, Reite E, Asherin R, Hernandez O: Meg auditory evoked fields suggest altered structural/functional asymmetry in primary but not secondary auditory cortex in bipolar disorder. Bipolar Disord 2009;11:371-381.

103 Edgar JC, Fisk CLt, Liu S, Pandey J, Herrington JD, Schultz RT, Roberts TPL: Translating adult electrophysiology findings to younger patient populations: Difficulty measuring 40-hz auditory steady-state responses in typically developing children and children with autism spectrum disorder. Developmental Neuroscience 2016;38:1-14.

104 Wilson TW, Hernandez OO, Asherin RM, Teale PD, Reite ML, Rojas DC: Cortical gamma generators suggest abnormal auditory circuitry in early-onset psychosis. Cerebral Cortex 2008;18:371-378.

105 Larsen KM, Pellegrino G, Birknow MR, Kjær TN, Baaré WFC, Didriksen M, Olsen L, Werge T, Mørup M, Siebner HR: 22q11.2 deletion syndrome is associated with impaired auditory steady-state gamma response. Schizophrenia Bulletin 2018;44:388-397.